Accounts

Conductive Copper Salts of 2,5-Disubstituted *N,N'*-Dicyanobenzoquinonediimines (DCNQIs): Structural and Physical Properties

Reizo Kato

RIKEN (The Institute of Physical and Chemical Research), 2-1 Hirosawa, Wako, Saitama 351-0198

(Received October 13, 1999)

Structural and physical properties of the Cu salts of a series of π-acceptors *N,N'*-dicyanobenzoquinonediimines (DCNQIs) are described. The most notable feature of this system is that 3d electrons in Cu interact with pπ electrons in DCNQI near the Fermi level. This unique feature has provided a lot of interesting solid state properties: the Mott transition triggered by the Peierls transition, the pressure-induced metal-insulator transition, the metal-insulator-metal (reentrant) transition, the three-dimensional Fermi surface, the anomalous isotope effects, the antiferromagnetic transition, the weak ferromagnetism, and the electron mass enhancement. The aim of this account is to give an overview of this unique pπ-d system.

Molecular conductors, whose roots go back to the discovery of organic semiconductors in 1954,[1] form one of the most attractive categories of materials. Studies of the metallic behavior followed by the charge density wave (CDW) transition observed in TTF-TCNQ[2] and the discovery of the first organic superconductor $(TMTSF)_2PF_6$, (TMTSF = tetramethyltetraselenafulvalene)[3] triggered new fields of solid state science. Recent advances in the studies of the magnetic quantum oscillations on molecular conductors have revealed that molecular conductors have *clear* electronic structures which can be well described by the simple tight-binding band calculation based on the extended Hückel approximation.[4] In most molecular metals, the conduction band originates from only *one* frontier molecular orbital (HOMO for donor, LUMO for acceptor). This is because the inter-molecular transfer energy is smaller than the energy differences among molecular orbitals. The clear electronic structure has enabled systematic understanding of a variety of exotic phenomena associated with low dimensionality: for example, CDW, Spin Density Wave (SDW), Spin Peierls transition, Field Induced Spin Density Wave (FISDW), and Angle Dependent Magneto Resistance Oscillations (AMRO). The simple tight-binding approximation, however, is not almighty, because the strong electron-electron correlation effect frequently plays an important role in molecular conductors. Even in such a case, a calculated Fermi surface is useful in understanding the anisotropy of intermolecular interactions, and physical and chemical modifications of the system can change the artificial Fermi surface into the real one. Molecular conductors can accept diverse chemical modifications, which provides the means of control of solid state properties.

In the majority of known molecular conductors, for example, TMTSF and BEDT-TTF (bis(ethylenedithio)-tetrathiafulvalene) salts, conducting properties are governed by organic pπ electrons. An introduction of metal d electrons into the pπ-electron system has been expected to provide a variety of new phenomena. In 1986, the Cu salt of 2,5-dimethyl-*N,N'*-dicyanoquinonediimine (DMe-DCNQI) was reported to exhibit extremely high electrical conductivity down to 1.3 K.[5] This was the first report on an anion radical salt which remains metallic down to very low temperature with no metal-insulator (M-I) transition. In the crystal of this salt, one-dimensional (1D) DCNQI columns are interconnected to each other through the Cu ions coordinated by the N atoms of four *N*-cyano groups, that is, the DCNQI molecule exhibits two faces: as "acceptor" and as "ligand". After this report, it was revealed that a series of 2,5-disubstituted *N,N'*-dicyanobenzoquinonediimines R_1,R_2-DCNQI (R_1, R_2 = CH_3, CH_3O, Cl, Br, I; Scheme 1) form 2 : 1 salts with various metal ions (Cu, Ag, Li, Na, K, NH_4, Rb, and Tl).[6] In these salts, except the Cu salts, the cations are considered simple monovalent ions and thus the formal charge of the DCNQI is −1/2, which means that conduction electrons originate in the 1D quarter-filled (organic) pπ band. On the other hand, the Cu salts have been revealed to be very unique pπ-d systems. A low-temperature X-ray diffraction study first suggested that the Cu ions in the metallic phase are situated in the mixed-valence state (Cu^+ : $Cu^{2+} \approx 2$: 1) and thus the

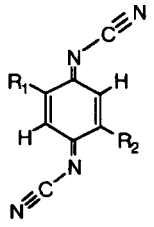

R_1,R_2-DCNQI

	R_1	R_2
DMeO-DCNQI	CH_3O	CH_3O
DI-DCNQI	I	I
MeI-DCNQI	CH_3	I
BrI-DCNQI	Br	Br
DMe-DCNQI	CH_3	CH_3
MeBr-DCNQI	CH_3	Br
DBr-DCNQI	Br	Br
MeCl-DCNQI	CH_3	Cl
DCl-DCNQI	Cl	Cl

Scheme 1.

3d electrons in Cu interact with the pπ electrons in DCNQI near the Fermi level.[7] This unique feature has provided a lot of interesting physical properties. The (DMe-DCNQI)$_2$Cu (DMe-salt) is the first molecular metal which possesses a three-dimensional (3D) Fermi surface.[8] The metallic state of the DMe-salt is easily suppressed by the application of pressure.[9] In the vicinity of the critical pressure, the metal-insulator-metal (reentrant) transition can be observed.[10] The choice of R_1 and R_2 also affects the electronic state.[11] The M-I transition in (DCNQI)$_2$Cu is accompanied by the CDW formation with three-fold periodicity and static charge ordering at the Cu sites ($\cdots Cu^{2+}Cu^{+}Cu^{+}\cdots$). The discovery of the deuteration-induced M-I transition in the DMe-salt[12] opened the way to the precise control of the electronic state by the selective deuteration, which led to fruitful physical investigations. The pressure and substituent effects can be understood in terms of the amount of charge transfer from Cu to DCNQI, which is sensitive to the coordination geometry around the Cu ion. However, the existence of one or more high-pressure metallic phase(s), typically observed in (DI-DCNQI)$_2$Cu (DI-salt; $R_1 = R_2 = I$), indicates that there should be other factors that affect the electronic state of the DCNQI-Cu system.

The present account describes many solid-state properties derived from the pπ-d interaction.

1. Preparation

Synthesis of DCNQI derivatives has been performed systematically by the German group whose report started in 1984.[13] The most convenient method is the one-step conversion from *p*-benzoquinones to *N*-cyanimines with bis(trimethylsilyl)carbodiimide. Another route starting from *p*-phenylenediamines is useful for the selective ^{15}N labeling of terminal cyanoimino (=N–CN) groups.

Site-selective isotope (D, ^{13}C, ^{15}N) substitution in the DCNQI molecule is of great importance in chemistry and physics of (DCNQI)$_2$Cu, because the isotope effect on the electronic state of the DMe-salt is drastic and provides a powerful means to tune the electronic state (see Sect. 3-4). Moreover, NMR-active ^{13}C and ^{15}N atoms afford significant information on the electronic state.[14]

The DMe-DCNQI molecule contains 8 hydrogen atoms, and 35 patterns of the selective deuteration are possible. The key step is synthesis of selectively deuterated xylenes with the ring deuteration and the methyl deuteration.[15] In order to introduce one deuterium atom into the six-membered ring, a H/D exchange reaction in the reduction step is used. A reductive deuteration of aromatic aldehyde (or ester) with $LiAlD_4$ and a reductive deuteration of chloro methyl group with superdeuteride lead to selectively methyl-deuterated xylenes. Combining all these methods, we find that almost all patterns of selective deuteration are possible.[15] The German group has reported other deuteration methods.[13c]

Terminal cyanoimino groups can be isotopically (^{13}C or ^{15}N) labeled by use of labeled bis(trimethylsilyl)carbodiimide as dicyanoimination reagent.[16] Selective ^{15}N-labeling is performed according to the *p*-phenylenediamine route. When $Pb(OAc)_4$ is used as the oxidant at the oxidation of dicyanodiamines to DCNQIs, the fragile C–N bonds are rearranged in a certain condition. (Diacetyliodo)benzene (DAIB) does not cause the migration of nitrogen and gave moderate yield.[16c]

Preparation of anion radical salts can be performed by several methods. For all the salts, electrochemical crystallization with constant current in acetonitrile is a very useful method. $[Cu(CH_3CN)_4]ClO_4$ or $CuBr_2$ is used as supporting electrolyte. A direct reaction of DCNQI with Cu metal in acetonitrile also gives the anion radical salt. As-prepared polycrystalline samples obtained by this method were used in the X-ray photoemission spectroscopy study (see Sect. 6). In the case of some Cu salts (especially the DMe-salt), large single crystals for physical measurements can be obtained with a slow diffusion of DCNQI and CuI in acetonitrile. Single crystals of the DMe-salt with high quality and moderate size are easily obtained with a reaction of DMe-DCNQI and $(n\text{-}Bu)_4NI$ in the presence of $(Et_4N)_2[CuBr_4]$ in acetonitrile. This reaction proceeds gradually and single crystals can be harvested within a day.

2. Room-Temperature Crystal Structure

All the Cu salts of R_1,R_2-DCNQI (R_1,R_2 = CH_3, CH_3O, I, Br, Cl) are isomorphous and have a tetragonal unit cell with space group of $I4_1/a$ (Fig. 1).[11] Planar DCNQI molecules are uniformly stacked along the tetragonal *c* axis. Each DCNQI molecule lies on the inversion center and a half of the DCNQI unit is crystallographically independent. Therefore, the unsymmetrical DCNQI molecules ($R_1 \neq R_2$) show an orientational disorder. The bond lengths in the DCNQI molecule vary according to the formal charge, which can be explained in terms of the coefficients of the LUMO of the neutral

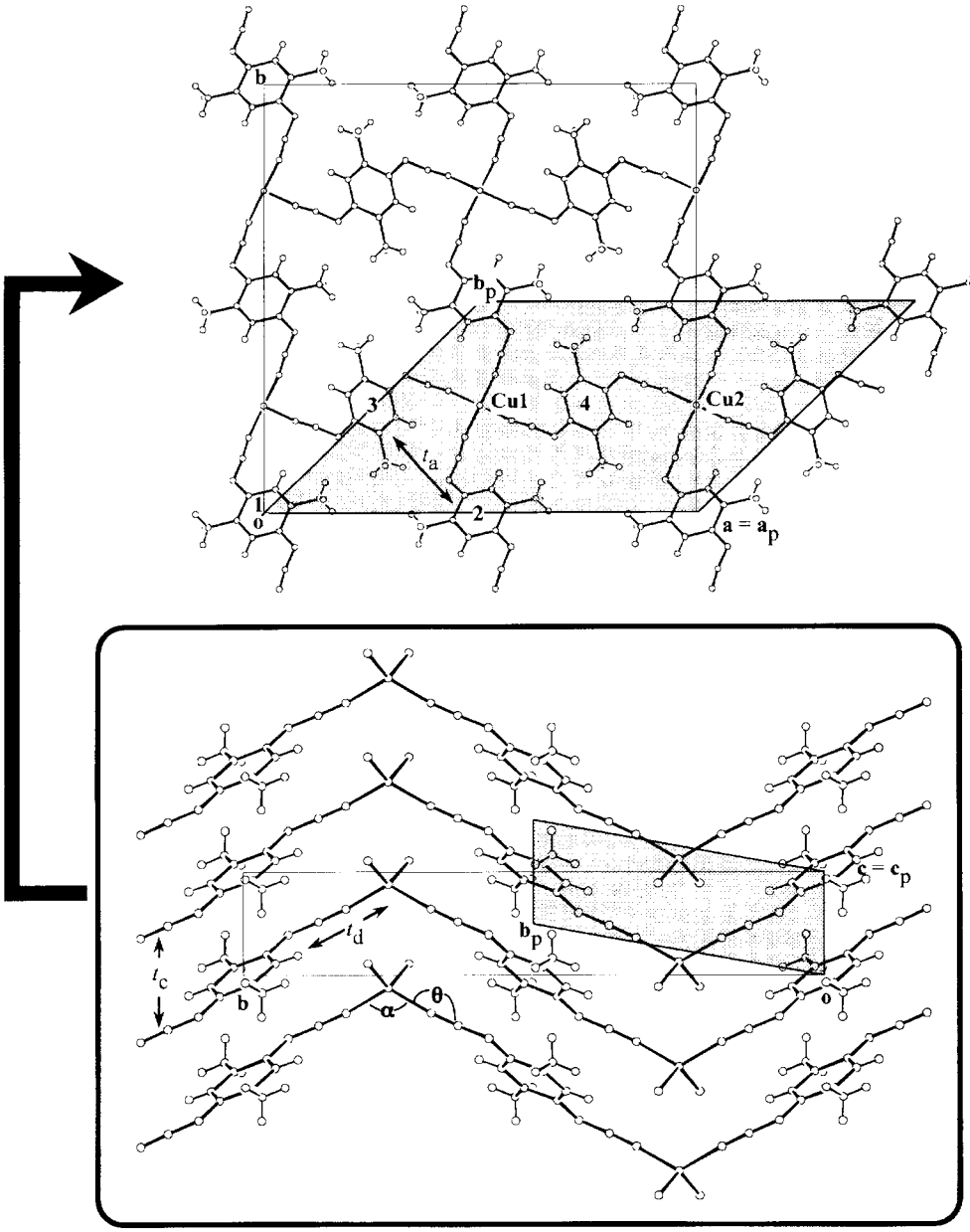

Fig. 1. Crystal structure of $(DMe\text{-}DCNQI)_2Cu$. A shaded cell is a primitive cell used for the band calculation (see Sect. 8-1).

molecule. The most significant variations are observed in the C=N–C part. Comparison of the bond lengths with those in the neutral unsubstituted DCNQI and in the isostructural Li salt suggests the notion of more than one-half unit negative charge per DCNQI unit in the Cu salts.[11] The interplanar distances between least-squares planes through the six-membered rings of the DCNQI units are in the range of 3.13—3.24 Å (Table 1). The overlap of the DCNQI molecules within a stack is of the usual "double bond over ring" type. Except for the case of the iodine-containing salts, each DCNQI column is separated from all others and there is no short inter-column contact. A significant feature of the iodine-containing salts is a very short inter-column I···I contact.[17] For example, in the DI-salt, the observed I···I distance 3.654 Å is 15% shorter than the van der Waals distance (4.30 Å). An introduction of bulky iodine atom(s) enhances the inclination of the DCNQI molecular plane with respect to the stacking axis (see ϕ values in Table 1), which is associated with an enlargement of the overlap displacement in the direction parallel to the long molecular axis and affects the coordination geometry around the Cu ion. The DI-salt exhibits unusual transport properties at the high-pressure region (see Sects. 3-1 and 3-2).

An essential structural feature is that the DCNQI columns are interconnected to each other through tetrahedrally coordinated Cu ions with local symmetry of D_{2d} (Fig. 1). The Cu ions are separated far from each other and there is no direct Cu···Cu contact. The significant coordination parameters (R, α, and θ) are listed in Table 1. The Cu–N distances (R) are comparable to those in the tetrahedral complex $[Cu(CH_3CN)_4]ClO_4$ (1.95—2.02 Å). The N–Cu–N angles (α) indicate the degree of distortion from the T_d symmetry. One can notice that, in the series of Cu salts with the (quasi)

Table 1. Structural Parameters of $(R_1,R_2\text{-DCNQI})_2Cu$

R_1,R_2-DCNQI	a/Å	c/Å	d/Å	ϕ/deg	R/Å	α/deg	θ/deg
DMeO-DCNQI	22.442(11)	3.839(1)	3.21	33.5	1.988(5)	126.0(2)	177.6(5)
DI-DCNQI	21.721(3)	4.096(1)	3.23	37.9	1.997(3)	122.3(2)	171.8(3)
BrI-DCNQI	21.631(2)	4.012(6)	3.22	36.6	1.987(5)	123.1(3)	170.6(5)
MeI-DCNQI	21.710(2)	3.988(1)	3.24	35.9	2.001(6)	123.6(4)	172.0(6)
DMe-DCNQI	21.613(3)	3.883(1)	3.18	33.8	1.986(1)	124.7(1)	170.6(1)
MeBr-DCNQI	21.601(6)	3.856(1)	3.18	34.6	1.979(2)	125.3(1)	168.6(2)
DBr-DCNQI	21.558(10)	3.896(1)	3.19	34.9	1.973(7)	125.3(3)	169.2(6)
BrCl-DCNQI	21.569(11)	3.845(1)	3.13	35.4	1.963(7)	126.1(3)	167.0(6)
MeCl-DCNQI	21.559(7)	3.823(2)	3.18	33.8	1.964(4)	126.2(2)	169.7(4)
DCl-DCNQI	21.55(2)	3.816(1)	3.16	34.1	1.972(5)	127.1(2)	168.1(4)

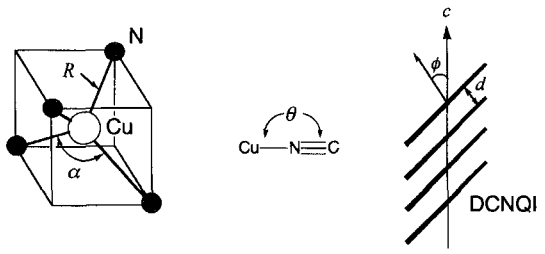

spherical substituents (Cl, Br, I, and CH_3), the larger substituent induces the smaller α values, that is, a reduction of the D_{2d} distortion. This α angle is one of important parameters which govern the electronic state (see Sect. 8-2). The Cu–N≡C angles (θ) fall within the range of 167.0—172.0°, except for that in $(DMeO\text{-}DCNQI)_2Cu$ (DMeO-salt; $R_1 = R_2 = CH_3O$; 177.6°). This distinctive θ value in the DMeO-salt is probably due to the non-spherical shape and larger size of the methoxy group. This difference in the θ value is related to a difference in the metal-ligand orbital overlapping[11] and gives the DMeO-salt an exceptional position in the DCNQI-Cu system. In this account, we focus our attention mainly on the DCNQI-Cu salts with the (quasi) spherical substituents.

Table 2. M-I Transition Temperature ($T_{M\text{-}I}$) and Critical Pressure ($P_{M\text{-}I}$) for $(R_1,R_2\text{-DCNQI})_2Cu$

		$T_{M\text{-}I}$ / K	$P_{M\text{-}I}$ / kbar
Group I	DMeO-DCNQI	—	8
	DI-DCNQI	—	15
	MeI-DCNQI	—	4
	BrI-DCNQI	—	3
	DMe-DCNQI	—	0.1
Group II	MeBr-DCNQI	155	—
	DBr-DCNQI	160	—
	MeCl-DCNQI	210	—
	BrCl-DCNQI	213	—
	DCl-DCNQI	230	—

3. Resistivity

3-1. Substituent Effect. Although $(R_1,R_2\text{-DCNQI})_2Cu$ salts are isomorphous, their physical properties are quite sensitive to the choice of R_1 and R_2 (Table 2).[18] According to conducting behavior at ambient pressure, they can be roughly classified into two groups. Group I salts are metallic down to a very low temperature, and group II salts undergo a sharp M-I transition at a rather high temperature (Fig. 2). In general, the Cu salts with bulky substituents belong to group I.

The DMe- and DMeO-salts are typical group I salts and exhibit almost identical temperature dependence of the resistivity. Resistivity is proportional to $T^{2.3}$ down to 30 K and remains almost constant below 15 K. The low-temperature conductivity reaches as high as 10^6 S cm^{-1}, which is one of the highest values for molecular conductors. No superconducting transition has been observed.

The DI-salt also belongs to group I, but its conducting behavior is different from that of above-mentioned group I salts.[19] The DI-salt is metallic down to 4.2 K at ambient pressure. The anisotropy of the resistivity is rather small ($\rho_{//c}/\rho_{\perp c}$ = 1 : 3). In the case of the DMe-salt, the ratio $\rho_{//c}/\rho_{\perp c}$ is about 1/10. From ca. 90 to 4.2 K, the resistivity is proportional to T^2, which suggests the existence of a strong electron-electron correlation (see Sects. 5-1 and 9-1).

The M-I transition of group II salts is accompanied by hysteresis, which indicates the first-order character. At the M-I transition temperature ($T_{M\text{-}I}$), a steep rise of the resistivity is observed. Both of the hysteresis and the steep rise grow faint as $T_{M\text{-}I}$ increases. The activation energy in the insulating region is less sensitive to the substituents (R_1 and R_2). $T_{M\text{-}I}$ is correlated to the bulkiness of the substituents, that is, the smaller substituent leads to the higher $T_{M\text{-}I}$. It has been mentioned that decreasing size of the substituents causes the increase of the N–Cu–N angle α, except for the DMeO-salt with the non-spherical substituents. Such a distortion of the coordination tetrahedron towards square planar symmetry can be caused by an application of pressure.

3-2. Pressure Effect. The group I salts exhibit a pressure-induced M-I transition, which is opposite to the

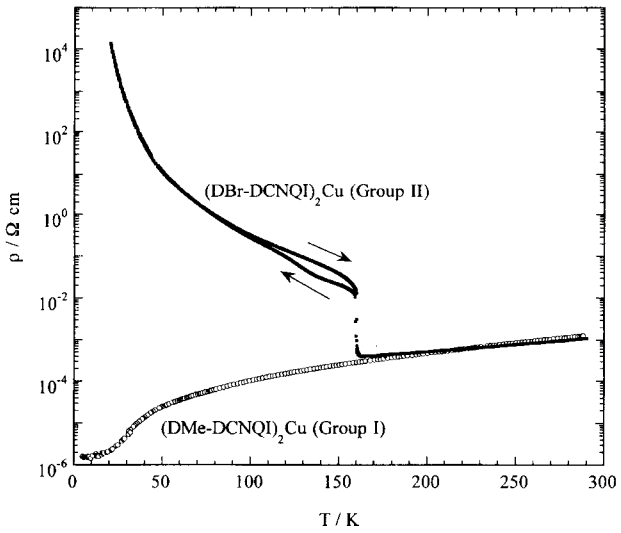

Fig. 2. Temperature dependences of the electrical resistivity ρ for the DMe- (group I) and the DBr- (group II) salts at ambient pressure.

case of conventional molecular conductors, for example $(TMTSF)_2X$. On the other hand, in the DCNQI salts with a monovalent cation (e.g. $(DMe\text{-}DCNQI)_2Ag$), the application of pressure expands a metallic region.[20] The critical pressure ($P_{M\text{-}I}$) depends on the substituents (R_1 and R_2), as shown in Table 2. The DMe-salt shows the lowest $P_{M\text{-}I}$, and its ambient-pressure metallic phase is suppressed by applying pressure as low as 100 bar.[10] This very low critical pressure of the DMe-salt leads to its unusual isotope effects (see Sect. 3-4). The higher pressure leads to the higher $T_{M\text{-}I}$ and the weaker first order character, whereas the activation energy remains constant. In the pressure region from 2 to 7.5 kbar, the M-I transition proceeds in two steps. The most striking feature is a restabilization of the metallic phase at low temperatures in the vicinity of the critical pressure (100—300 bar).[10] For example, at 150 bar, the system shows a sharp resistivity jump followed by an abrupt return to the metallic state with lowering temperature. The temperature dependence of the resistivity is similar above and below the narrow temperature region where the system becomes an insulator, which suggests that the reentrant metallic state is of the same nature as the high-temperature metallic state. Hereafter, we classify the Cu salts showing the reentrant transition into group III. The reentrant transition is also observed in the DMeO-salt in the pressure region of 8—10 kbar, but the recovery of the metallic conductivity is not complete.[21] The critical pressure of the DMeO-salt (8 kbar) is higher than that of the DMe-salt. The resistivity behavior above 10 kbar is similar to that of the group II salts.

The pressure effect on the group II salt was investigated in $(MeBr\text{-}DCNQI)_2Cu$ (MeBr-salt; $R_1 = CH_3$, $R_2 = Br$) with $T_{M\text{-}I}$ of 155 K at ambient pressure (Fig. 3).[22] Pressure dependence of the room temperature resistivity shows a minimum around 2 kbar. $T_{M\text{-}I}$ increases with increasing pressure. Around 3 kbar, a stepwise M-I transition is observed. The transition becomes broad and sluggish at high pressures.

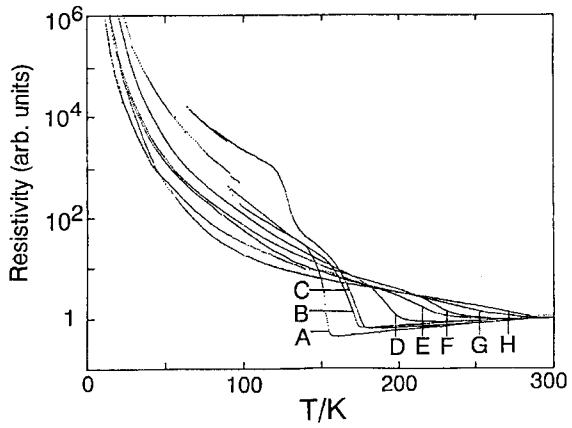

Fig. 3. Temperature dependence of the electrical resistivity ρ for $(MeBr\text{-}DCNQI)_2Cu$ under pressure. A = 1 kbar; B = 3 kbar (cooling process); C = 3 kbar (heating process); D = 4 kbar; E = 6 kbar (cooling process); F = 6 kbar (heating process); G = 10 kbar; H = 15 kbar.

Above 10 kbar, the resistivity shows only monotonous increase from room temperature.

The above results related to the substituent and pressure effects can be summarized qualitatively (and roughly) in a generalized pressure (P)–temperature (T) phase diagram (Fig. 4). The system turns from the group I to the group II by the application of pressure. The group III salts are located in the vicinity of the critical pressure. The physical pressure can be replaced by the substituent effect ("chemical" pressure), and they are unified into "effective" pressure. Although the chemical pressure is not completely equivalent to the physical pressure, both of them affect the coordination geometry around the Cu ion similarly.

The P–T phase diagram in Fig. 4 should be modified in the higher-pressure region, depending on the substituents (R_1

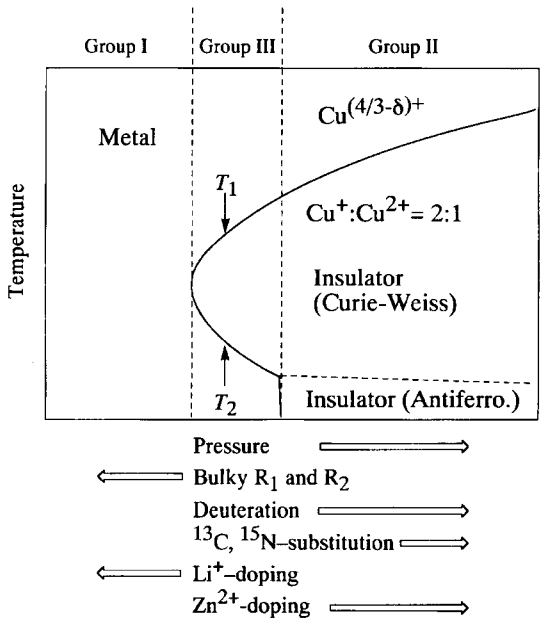

Fig. 4. Schematic "effective pressure"–temperature phase diagram (see Sect. 4).

and R_2). The first and typical example is the DI-salt.[19] Figure 5 shows temperature dependence of the electrical resistivity along the c axis of the DI-salt under pressure. The room temperature resistivity shows monotonous decrease with increase in pressure. In the low pressure region (< 15.1 kbar), the DI-salt remains metallic down to 4.2 K. Since the residual resistivity is hardly affected by pressure, the $\rho_{R.T.}/\rho_{4.2\ K}$ ratio decreases with increase in pressure. Above 15.3 kbar, a sharp M-I transition appears with hysteresis (Fig. 5a). The critical pressure $P_{M\text{-}I}$ for the DI-salt is the highest in the group I salts. This corresponds to the smallest α value. $T_{M\text{-}I}$ changes sensitively near $P_{M\text{-}I}$. As pressure increases, $T_{M\text{-}I}$ shifts positively and the resistivity jump at $T_{M\text{-}I}$ is gradually suppressed. In the DI-salt, the reentrant transition has never been observed. This may suggest that the reentrant pressure region is very limited. The most remarkable feature is that the M-I transition is suppressed above ca. 20 kbar. In this pressure region (ca. 20—22 kbar), the system remains metallic down to ca. 180 K, and shows a resistivity maximum around 120 K, followed by the metallic behavior. There is little hysteresis, which indicates the second order character of the transition. On the other hand, in the DMe-salt, the high pressure up to 20 kbar only enhances the semiconductive behavior.[19] The high-pressure metallic phase above 20 kbar in the DI-salt is the first such observation in the DCNQI-Cu salts. The resistivity behavior of the DI-salt under pressure higher than ca. 25 kbar is more complicated. The M-I transition appears again around 25 kbar. This transition exhibits little hysteresis and is suppressed above ca. 35 kbar (Fig. 5b).

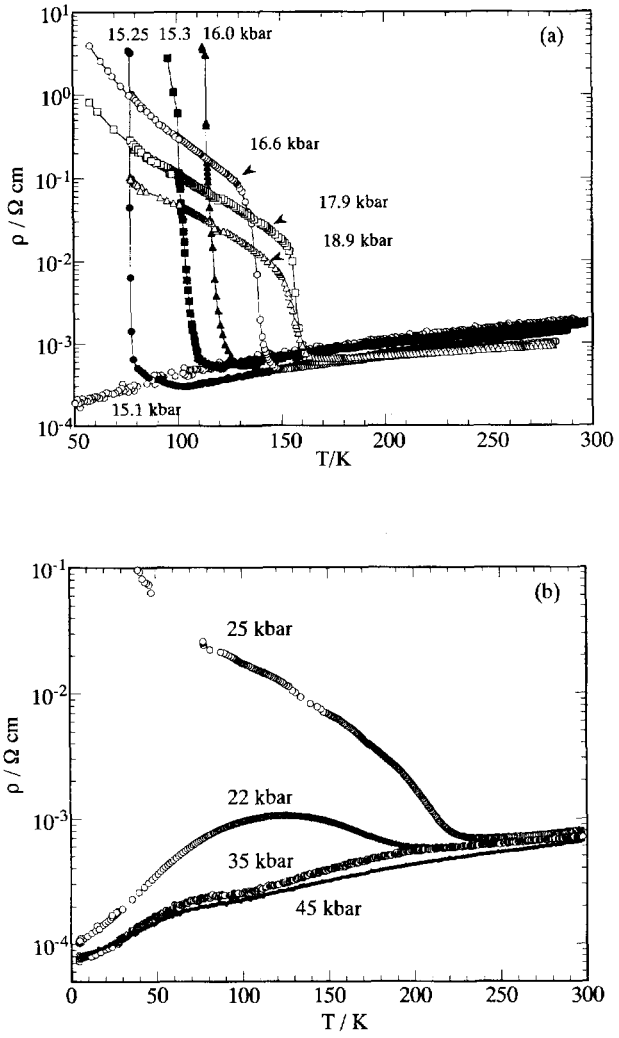

Fig. 5. Temperature dependence of the electrical resistivity ρ for (DI-DCNQI)$_2$Cu under pressure. (Reproduced from Fig. 2 in Ref. 17a.

The BrI-salt (R_1 = Br, R_2 = I) also shows a complicated pressure effect similar to that in the DI-salt.[17] This system shows a clear reentrant transition in the vicinity of $P_{M\text{-}I}$, as is often observed in other group I salts under pressure. Very recently, the DBr-salt (group II) has been found to show a metal-like behavior, like the BrI-salt in the high-pressure region.[23] This is in contrast to the behavior of the MeBr-salt. The MeI-salt (R_1 = CH_3, R_2 = I) remains metallic at ambient pressure and shows a pressure-induced M-I transition accompanied by a clear reentrant behavior. The high-pressure metallic phase, however, has never been found in the MeI-salt.[17b]

3-3. Alloy Effect. An attempt to observe the reentrant transition at ambient pressure was performed in an alloy of the group I and the group II, [(DMe-DCNQI)$_{1-x}$(MeBr-DCNQI)$_x$]$_2$Cu.[24] This alloy system was prepared electrochemically. The modes of the temperature dependence of the resistivity can be classified into the following four types: (I) $x < 0.1$; The reentrant behavior is observed. The residual resistivity increases rapidly with x, which indicates strong disorder effect. (II) $0.1 < x < 0.6$; The resistivity shows large hysteresis. In the cooling process, the resistivity shows metallic behavior down to ca. 90 K, followed by an almost discontinuous increase, whereas the system remains low conductive up to ca. 210 K in the warming process. (III) $x \approx 0.7$; The system is semiconductive for all over the temperature range, which may be ascribed to the electron localization due to the severe lattice disorder. (IV) $x > 0.8$; A sharp M-I transition similar to that of the pure MeBr-salt is observed. The x dependence of the N–Cu–N angle (α), determined by the X-ray crystal structure analysis, shows that α increases stepwise with increasing x. There are three regions: small-α region ($x < 0.1$), intermediate-α region ($0.1 < x < 0.6$) and large-α region ($x > 0.8$). The reentrant behavior is observed in the small-α region. It should be noted that the replacement of DMe-DCNQI with MeBr-DCNQI enlarges the cell volume, whereas the application of pressure leads to the reduction of the unit cell volume. This indicates that an essential factor of the metal instability is not the reduction of the cell volume but the enlargement of the α value.

Another type of alloy can be obtained by the Li doping at the Cu site. Especially, the Li doping in the group II salts is very interesting. The pure Li salt is isostructural with the Cu salt. Since the difference between the crystal structures of the Cu and Li salts is not so large, the Li^+ ion is expected to replace the Cu ion without serious structural disturbance. The special feature of the Li doping is the continuous change

of the formal charge of the DCNQI molecule, which was confirmed by x-dependence of the C=N (imine) stretching frequency of DCNQI in (MeBr-DCNQI)$_2$Cu$_{1-x}$Li$_x$.[25] The Li$^+$-doping stabilizes the metallic state, that is, the Li$^+$-doping corresponds to negative pressure. $T_{M\text{-}I}$ values of (MeBr-DCNQI)$_2$Cu$_{1-x}$Li$_x$ decrease rapidly with increasing x ($x <$ 0.2), and the system with $0.25 < x < 0.50$ is metallic down to 4.2 K. In the case of (DBr-DCNQI)$_2$Cu$_{1-x}$Li$_x$, the M-I transition is also suppressed by the Li-doping, and the reentrant behavior is observed in the concentration range of $0.1 \leq x \leq 0.23$.[26] These results are not trivial, considering that the pure Cu and Li salts are both insulating in the low-temperature region. The Li-doping in the group I salts only increases the residual resistance due to randomness.

Doping of divalent cations is very difficult. For example, the Zn^{2+}-doping is possible only when the Zn content is very low, and obtained crystals have poor quality. Interestingly, (DMe-DCNQI)$_2$Cu$_{0.97}$Zn$_{0.07}$ shows the weak reentrant behavior, which suggests that the Zn^{2+}-doping corresponds to positive pressure.[27] The Li$^+$ and Zn^{2+} doping effects will be discussed again in Sect. 8-2.

3-4. Isotope Effect. The reentrant transition was first observed in the DMe-salt under very low-pressure generated by the He-gas pressure technique. The reentrant transition is also observed in some alloy systems at ambient pressure. But, technical problems in the pressure experiment or serious disorder effect in the alloy system hindered detailed studies. The first breakthrough was done by the German group.[12] They found a M-I transition induced by methyl- and full deuteration in (DMe-DCNQI-d$_n$)$_2$Cu (n = 3,6,8). This remarkable isotope effect gave us a suggestion that electronic state can be controlled by the number and position of deuterium atoms in a wide range of the effective pressure (from the group I to the group II). It should be added that among the DCNQI-Cu salts, the DMe-salt can provide single crystals with the largest size and high quality. Hereafter, we use a notation $-$d$_n$[a_1,a_2;b] ($0 \leq a_1$, $a_2 \leq 3$, $0 \leq b \leq 2$), where a_1 and a_2 are numbers of deuterium atoms in each methyl group and b is that in the six-membered ring, for the simplified expression of the selectively deuterated DMe-system with n deuterium atoms in total. Non- and fully-deuterated systems are simply represented as –h and –d$_8$, respectively. Transition temperatures obtained in the resistivity measurements are drastically changed by the number and position of deuterium atoms (Table 3).[15] Especially, in the –d$_3$[1,0;2], –d$_2$[1,1;0], –d$_2$[2,0;0], –d$_3$[1,1;1], –d$_4$[1,1;2], and –d$_3$[3,0;0] salts, a giant reentrant transition can be observed (Fig. 6). This is the first ambient-pressure reentrant transition observed in a non-alloy system. Comparison of transition temperatures with those in the –h system under pressure[10] suggests that the effect of deuteration can be converted into pressure. This "effective pressure" P_{eff} (bar) is approximately expressed as a linear function of a_1, a_2, and b,

$$P_{eff} \approx 80\{(a_1 + a_2) + 0.2b\}.$$

This formula indicates that

Table 3. Transition Temperatures for Selectively Deuterated (DMe-DCNQI-d$_n$)$_2$Cu (see Fig. 4)

	Transition temperature				
	On cooling		On warming		
–d$_n$	T_1	T_2	T_1	T_2	P_{eff} / bar[a]
–h	—	—	—	—	(0)
–d$_1$[0,0;1]	—	—	—	—	16
–d$_2$[0,0;2]	ca. 40 (slight sh)[b]		ca. 50 (slight sh)[b]		32
–d$_1$[1,0;0]	ca. 40 (sh)[b]		ca. 50 (sh)[b]		80
–d$_2$[1,0;1]	ca. 40 (sh)[b]		ca. 50 (sh)[b]		96
–d$_3$[1,0;2][c]	51	28	54	41	112
–d$_2$[1,1;0]	55	21	56	35	160
–d$_2$[2,0;0]	55	20	58	35	160
–d$_3$[1,1;1]	57	16	63	30	176
–d$_4$[1,1;2]	61	13	59	33	192
–d$_3$[3,0;0][d]	62	10	66	22	240
	64	—	67	—	
–d$_5$[3,0;2]	66	—	70	—	272
–d$_4$[2,2;0]	68	—	71	—	320
–d$_6$[3,3;0]	75	—	78	—	480
–d$_7$[3,3;1]	77	—	80	—	496
–d$_8$	80	—	82	—	512

a) Calculated from $P_{eff} \approx 80\{(a_1 + a_2) + 0.2b\}$ (see Sect. 3-4). b) sh stands for shoulder. Some samples do not indicate any anomaly. c) Some samples indicate no giant reentrant transition, but only a shoulder at ca. 50 K. d) Some samples do not indicate the reentrant transition.

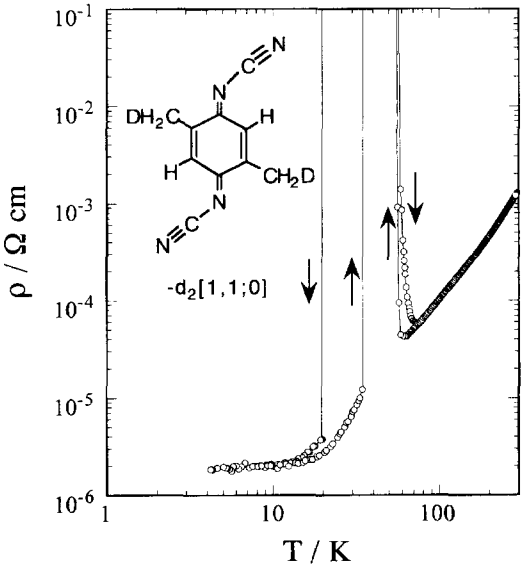

Fig. 6. Reentrant transition observed in the electrical resistivity ρ for (DMe-DCNQI–d$_2$[1,1;0])$_2$Cu.

(1) the deuteration at the methyl group is more effective, and

(2) the substitution pattern is not significant (for example, both the –d$_2$[1,1;0] and the –d$_2$[2,0;0] systems show very similar behavior).

Unit cell parameters of the selectively deuterated systems were carefully determined using non-monochromatized Mo $K\alpha_1$ radiation at room temperature. The results indicate a tendency of the unit cell contraction by the deuteration.[8b]

This comes mainly from the fact that the C–D bond is slightly shorter than the C–H bond as a result of the lower zero point energy and unharmonic term in the potential curve. This steric isotope effect makes each DMe-DCNQI molecule a bit less bulky and leads to 'contraction' of intermolecular distances. This situation is similar to that under pressure. In this sense, the deuteration is equivalent to the application of pressure. In the crystal, the bulky methyl groups contact to each other along the stacking c axis and the inter-molecular distance is mainly affected by repulsion between the methyl groups. Therefore, the methyl deuteration is more effective than the ring one. The ring deuteration has a much smaller but measurable effect. This would be explained from the rather short distance between the ring hydrogen and the terminal cyano nitrogen of the neighboring molecule.

The coordination geometry around the Cu ion is correlated to the stability of the metallic state in the DCNQI-Cu system (see Sect. 8-2). The application of (effective) pressure is considered to enhance the distortion of the coordination tetrahedron. Unfortunately, the accuracy of the X-ray crystal structure analysis at room temperature is not enough to detect changes in the significant coordination parameters (R, α, and θ) for the selectively deuterated system.

Since the DMe-salt gives large single crystals with high quality and the deuteration does not affect the crystallization process of the Cu salt, alloy systems derived from deuterated DMe-DCNQI molecules have provided much clearer information. Details of the phase diagram for the DMe-salt were investigated with use of the alloy system [(DMe-DCNQI-h)$_{1-x}$(DMe-DCNQI-d$_8$)$_x$]$_2$Cu.[28] Since the difference between –h and –d$_8$ molecules is very small, this system is a homogeneous alloy where the effect of disorder is reduced to a minimum. The x–T phase diagram reproduces the low-pressure region (1—500 bar) in the P–T phase diagram. One of the important features is a sharp vertical boundary line between the insulating and low-temperature metallic phases (Fig. 4). That is, the I→M transition temperature T_2 in the reentrant region sharply drops to 0 K near the (antiferromagnetic) insulator phase.

The Li-doped group II system (DMe-DCNQI-d$_7$[3,3;1])$_2$Cu$_{1-x}$Li$_x$ forms a good solid solution in the low-Li content region ($x < 0.1$).[27] This alloy system was prepared by the gradual reduction of DCNQI with (n-Bu)$_4$NI in the presence of (Et$_4$N)$_2$[CuBr$_4$] and LiClO$_4$. In the concentration region of $0.038 < x < 0.052$, the giant reentrant transition is observed, as in group III. Compared with (DBr-DCNQI)$_2$Cu$_{1-x}$Li$_x$, this system shows much sharper reentrant transition in the lower Li-content region. The larger contents of Li$^+$ ($0.055 \leq x \leq 0.1$) stabilize the metallic state down to 4.2 K. The Zn^{2+}-doping in the group II salt was first performed in (DMe-DCNQI-d$_7$[3,3;1])$_2$Cu$_{0.97}$Zn$_{0.03}$ where the Zn^{2+}-doping slightly raises $T_{M\text{-}I}$. This also indicates that the Zn^{2+}-doping corresponds to positive pressure.

An unexpected isotope effect in the ^{13}C-substitued DMe-salt was found during the NMR study.[16a] The ^{13}C-labeling of two cyano groups was carried out for the non-deuterated (–h) and selectively deuterated (–d$_1$[1,0;0] and –d$_2$[2,0;0]) DMe-DCNQI molecules. Isotope purity for ^{13}C was higher than 98 atom%. FT-IR spectra of neutral molecules showed an isotopic shift of the C≡N stretching vibrational frequency (ca. 50 cm^{-1}). Resistivity measurements for each Cu salt have revealed that the ^{13}C-substitution increases "effective pressure" by ca. 100 bar (Fig. 7). On the other hand, the ^{13}C-labeling for the methyl carbon shows only a negligibly small effect.

Furthermore, replacement of all four N atoms in the –h and –d$_4$[1,1;2] DMe-DCNQI molecules with ^{15}N atoms was found to cause the same isotope effect (Fig. 7). In this case, an increase in the effective pressure (ca. 90 bar) is slightly smaller than that in the ^{13}C-substitution. Two patterns of the selective ^{15}N-labeling of the terminal cyanoimino groups, ^{15}N atoms to inner imino-N atoms (in-^{15}N$_2$) and to outer cyano-N atoms (out-^{15}N$_2$), were carried out for (DMe-DCNQI–d$_2$[1,1;0])$_2$Cu whose transition temperatures are very sensitive to the effective pressure.[29] Other patterns of isotope labeling in (DMe-DCNQI–d$_2$[1,1;0])$_2$Cu, ^{13}C atoms to cyano-C atoms (^{13}C$_2$) and ^{15}N atoms to all four N atoms (^{15}N$_4$), were also examined for comparison. Intensity of the isotope effect appears in the order of ^{13}C$_2$ > ^{15}N$_4$ > in-^{15}N$_2$ ≥ out-^{15}N$_2$. The origin of this unusually large heavy-atom isotope effect remains an open question.

4. Low-Temperature Crystal Structure

The chemistry and physics of the DCNQI-Cu salts as a unique pπ-d system were initiated by one X-ray oscillation photograph which exhibits three-fold superlattice reflections from (MeCl-DCNQI)$_2$Cu (MeCl-salt; R$_1$ = CH$_3$, R$_2$ = Cl) below $T_{M\text{-}I}$.[7] The development of the three-fold superstructure ($a \times b \times 3c$) in the insulating phase strongly suggests the mixed valence state of Cu in the metallic phase.[7] In usual 1D metals, the M-I transition accompanied by CDW originates in a divergence of the density response function by a weak perturbing potential with the wave number $Q = 2k_F$, where

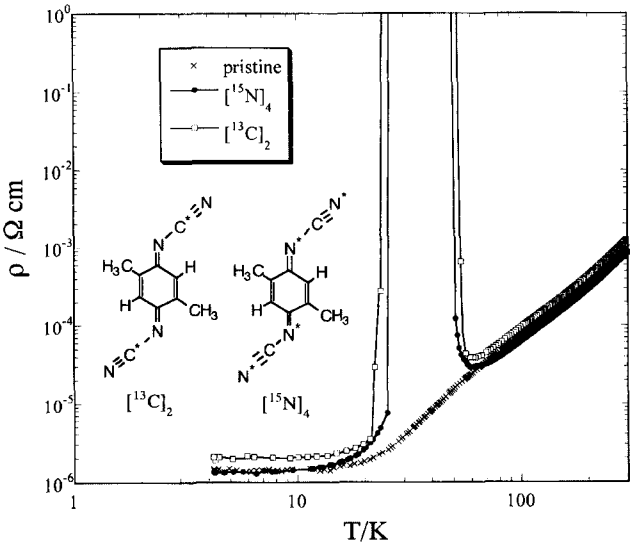

Fig. 7. ^{13}C- and ^{15}N-isotope effect on the electrical resistivity ρ of (DMe-DCNQI-h)$_2$Cu (cooling process).

k_F is the Fermi wave number.[30] If the Cu ion is monovalent, the formal charge of the DCNQI is $-1/2$ and thus the 1D pπ band is quarter-filled ($k_F = \pm\pi/4c$). Therefore, the periodicity of the lattice distortion is $2\pi/Q = 4c$. In the presence of strong on-site Coulomb repulsion between electrons, the band splits into the so-called upper and lower Hubbard bands. They halve the electrons which the original band can accommodate. Therefore, when electrons are accommodated only in the lower band, the Fermi wave number is twice as large as k_F for non-interacting electrons. In this case, the CDW formation is possible, but the wave number of the perturbing potential is $4k_F$. Under this $4k_F$ CDW state, there remains a spin degree of freedom. The spin system can form an antiferromagnetic state at lower temperature. When the lattice is allowed to modulate with the wave number $2k_F$ to make electron pairs, however, the system undergoes a transition to a state with a total spin = 0. This is a spin-Peierls transition. If there is strong long-range Coulomb repulsion between electrons, there is another possibility of the $4k_F$ instability, the $4k_F$ Wigner crystallization. The Ag salts of DMe-DCNQI and DI-DCNQI are two typical examples. (DMe-DCNQI)$_2$Ag exhibits diffuse lines with $q = c^*/2$ (corresponding to $4k_F$) at room temperature.[31] This diffuse scattering transforms into satellite reflections below 100 K. At 83 K, the system undergoes a second-order transition accompanied with the formation of satellite reflections at $q = (0,0,c^*/4)$. Transport properties and magnetic susceptibility indicate that these behaviors can be interpreted in terms of the $4k_F$ CDW formation followed by the spin-Peierls transition. On the other hand, for (DI-DCNQI)$_2$Ag, periodic molecular deformation possibly related to molecular valence ordering has been found from $4k_F$ satellite reflection intensity distribution in q-space.[32] This can be ascribed to the Wigner crystal formation.

The Cu salts, however, exhibit satellite reflections at $q = (0,0,c^*/3)$, indicating that the 1D band is 1/3-filled and thus the valence of DCNQI is $-2/3$. Temperature dependence of the satellite peak intensities in the MeBr-salt was investigated with use of the four-circle diffractometer.[11] The satellite reflections develop discontinuously at $T_{M\text{-}I}$, and the absence of the diffuse lines above $T_{M\text{-}I}$ indicates that the M-I transition in the Cu salts is not a simple CDW transition.

For the entire group II salts investigated (MeCl–,[7] and MeBr-salts,[11] and the alloy [(DMe-DCNQI)$_{0.9}$(DBr-DCNQI)$_{0.1}$]$_2$Cu[22]), the periodicity of the lattice distortion is $3c$. For the group I salts (DMe- and DI-salts), the high-pressure X-ray diffraction study has revealed that the insulating state under pressure is also accompanied by the three-fold superlattice.[33] The reentrant transition of the group III salts was investigated by the monochromatic Laue photograph method for the deuterated DMe-salts: [(DMe-DCNQI-h)$_{1-x}$(DMe-DCNQI-d$_8$)$_x$]$_2$Cu ($x = 0.29$ and 0.26)[34] and (DMe-DCNQI–d$_2$[1,1;0])$_2$Cu.[35] In the M-I transition of the group III salts, the three-fold superlattice is also observed with no precursor diffuse scattering. These three-fold superlattice spots disappear in the reentrant metallic phase. Furthermore, the Li-doped system (DMe-DCNQI-d$_7$[3,3;1])$_2$Cu$_{1-x}$Li$_x$ ($x = 0.04$) which belongs to group III also exhibits a three-fold superlattice in the insulating state which disappears in the reentrant metallic state.[27] All these results indicate that the three-fold superstructure is a common feature of the insulating state of the DCNQI-Cu salts.

Temperature dependence of the lattice constants was measured for the DMe-, MeBr-, DBr-, MeCl-, and BrCl–salts.[11] For all the salts, the lattice constant a shows a negative thermal expansion, whereas the thermal expansion of the c axis is normal. The lattice constants of the DMe-salt (group I) show no anomaly throughout the entire range of temperature investigated (from room-temperature to 100 K). The group II salts clearly exhibit an abrupt decrease in the c-axis length at $T_{M\text{-}I}$. The magnitude of the decrease in the c-axis length at $T_{M\text{-}I}$ seems to become large with lowering $T_{M\text{-}I}$.

The low-temperature crystal structures (the average structures for the insulating phase) were determined with use of the four-circle diffractometer (cold N_2 stream from liquid N_2) or the Weisenberg-type imaging plate (closed-cycle helium refrigerator). The most prominent feature is that the N–Cu–N angle α increases gradually with lowering temperature and shows an abrupt increase at $T_{M\text{-}I}$ (Fig. 8).[11,36] This suggests that the M-I transition can be described as a cooperative structural transition associated with the CDW instability of the DCNQI column and the intensive deformation of the coordination tetrahedron around the Cu ion. In the group III salt (DCNQI–d$_2$[1,1;0])$_2$Cu, across the I-M transition, the α value drops into the same value that the group I salt reaches (Fig. 8).[36] These results indicate that the α angle is closely related to the electronic state of the DCNQI-Cu salts. It should be noted that the magnetic structure in the insulating state can be derived from the average structure (see Sect. 5-2).

X-Ray crystal structure analysis of the three-fold insulating phase was tried for the MeBr-salt at 110 K.[22] The extinction rule of the superlattice reflections indicates that the three-fold structure does not have a body-centered lattice and there must be Cu atoms (and/or DCNQI molecules) interrelated by

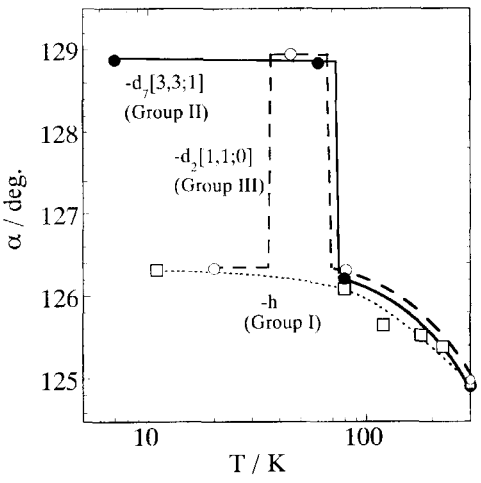

Fig. 8. Temperature dependences of the N–Cu–N coordination angle α in the selectively deuterated DMe-salts (groups I, II, and III).

body-centered translational symmetry, whose positions are modulated in the anti-phase fashion. The space group $P\bar{4}$ was assumed because of the requirement of the "anti-phase modulation". Since the intensities of superlattice reflections were very weak, the usual procedure could not be used and the DCNQI molecules were refined assuming rigid bodies. This analysis provides important information on the arrangement of the Cu ions, but the information on the coordination geometry around the Cu ion could not be determined accurately.

5. Magnetic Properties

5-1. Static Magnetic Susceptibility. Magnetic properties are very important in the description of the DCNQI-Cu salts. The M-I transition in this system is not a simple CDW transition, but a magnetic transition associated with the appearance of the local magnetic moments on the Cu sites. This point was noticed in the ESR measurements for the MeBr- and MeCl-salts in the insulating phase.[37] The *g*-factor (*H*//*c*) suggests that the ESR signal in the insulating phase originates from only Cu^{2+}. The intensity is consistent with the spin density deduced from the Cu^{+} : Cu^{2+}ratio = 2 : 1. From the magnetic viewpoint, the M-I transition of this system is characterized by the abrupt change of Cu 3d electrons from the itinerant state to the localized state.

The fully deuterated DMe-salt (DMe-DCNQI-d_8)$_2$Cu is the most suitable example for the study of the magnetic aspects of the group II salts, because it affords satisfactory large single crystals. Figure 9a shows temperature dependence of the static magnetic susceptibility.[38] In the metallic phase, temperature-independent Pauli-like behavior is observed. At $T_{M\text{-}I}$ (= 80 K), there is a jump of susceptibility. It should be recalled that the ordinary CDW transition leads the system to the non-magnetic state. This susceptibility jump indicates an appearance of local spins. These local spins obey the Curie–Weiss law down to ca. 30 K. The Curie constant indicates that one-third of the total Cu is Cu^{2+} ($S = 1/2$). At 8 K, the antiferromagnetic transition occurs. The spin-flop type magnetization curve for the fields perpendicular to the *c* axis and anisotropy of the susceptibility indicate that the Cu spins are aligned in the *ab* plane, that is, the easy axis is in the *ab*-plane and the *c*-axis is the hard axis. It should be noted that around the Néel temperature T_N an enhancement of susceptibility is observed when the field is applied perpendicular to the *c* axis, whereas there is no anomaly when the field is applied along the *c* axis. Non-linear field dependence of magnetization, hysteretic magnetization curve, and thermoremanent magnetization observed perpendicular to the *c* axis indicates that spontaneous magnetization perpendicular to the *c* axis appears below 8 K and shows a maximum at ca. 7 K. This weak ferromagnetism can be explained by the canting of the antiferromagnetic spins. The ferromagnetic saturation moment is very small ($5\times10^{-4}\mu_B/Cu^{2+}$), which involves small inclination (ca. 10^{-2} deg.) of the spins from the antiparallel alignment. Similar weak ferromagnetism is observed also in the DBr-salt (T_N = 16 K) below 16 K.[39] The ferromagnetic component for (DMe-DCNQI-d_8)$_2$Cu disappears at ca. 2 K, whereas that of the DBr-salt tends to saturate below ca. 8 K.

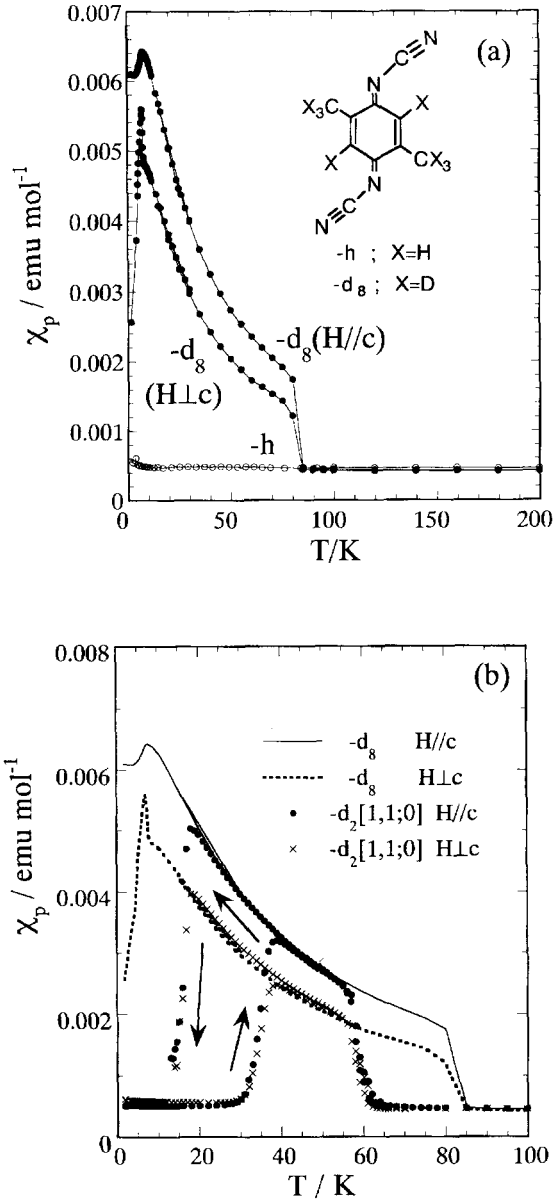

Fig. 9. Temperature dependences of the paramagnetic susceptibility χ_p for the selectively deuterated DMe-salts (groups I, II, and III).

The detailed magnetic susceptibility measurement for the group III salt has become possible by the selective deuteration. In this case, one should pay attention to the strong overcooling effect. It takes a long time for the system to reach thermal equilibrium. This effect tends to suppress the susceptibility in the insulating phase and enhance the susceptibility in the reentrant metallic phase. An overnight annealing removed this overcooling effect. Figure 9b shows temperature dependence of the paramagnetic susceptibility χ_p of (DMe-DCNQI-d_2[1,1;0])$_2$Cu.[40] The insulating phase exhibits the Curie–Weiss-like χ_p identical with those of the group II salts. The reentrant metallic phase shows the same Pauli-like χ_p as that of the high-temperature metallic phase,

which indicates that both metallic phases are identical to each other.

In the metallic state, some DCNQI-Cu salts, for example, the (deuterated and non-deuterated) DMe-, DMeO-, DBr-salts show temperature independent Pauli-like susceptibility ($4.3—5.6\times10^{-4}$ emu mol^{-1}, Fig. 9a).[41] On the other hand, the static magnetic susceptibility of the DI-salt is 2—3 times as large as those of the above-mentioned Cu salts.[42] The temperature dependence of the paramagnetic susceptibility has a broad maximum around 110 K (Fig. 10). The MeI- and BrI-salts, where one of the iodine atoms in the DI-salt is replaced with a methyl group and a bromine atom respectively, exhibit χ_p values intermediate between those of the DMe- and DI-salts, with a broad maximum around 200 K.[43] From the viewpoint of the phenomenological theory of itinerant electron magnetism,[44] the temperature where χ_p exhibits the maximum (T_{max}) can be related to the characteristic temperature of spin fluctuation. In this framework, T_{max} is proportional to $1/\chi_0$, where χ_0 is the susceptibility at 0 K. This relation seems to be satisfied in the present system. If the spin fluctuation mechanism is applicable, T_{max} is a measure of effective pπ-d hybridization determining the width of peak structure of a narrow band near the Fermi level. T_{max} values for the iodine-containing salts indicate reduction of the effective pπ-d hybridization (see Sect. 9-1).

5-2. NMR. In NMR measurements, one can obtain information about the electronic spin susceptibility from the Knight shift (shift of the resonance frequency from that for an isolated nucleus) and that about the metallic character of conduction electrons and the electron–electron Coulomb repulsion from the relaxation rate.[30] The DCNQI-Cu system has a 1D Fermi surface associated with the DCNQI column and a 3D Fermi surface derived mainly from the Cu 3d orbital (see Sect. 8-1). Therefore, it seems very likely that the ^{1}H nucleus probes the 1D pπ band mainly, whereas the ^{63}Cu nucleus probes the 3D pπ-d hybridized band.

The ^{1}H-nuclear-spin-lattice relaxation rate T_1^{-1} of the DBr-salt (group II) in the metallic state obeys the Korringa-law (T_1T = const.)[30] which holds in uncorrelated Fermi liquid systems. The relaxation mechanism in the metallic state is governed by the hyperfine coupling with conduction electrons of the pπ-band. At $T_{M\text{-}I}$, T_1^{-1} shows a discontinuous increase, which reflects the appearance of localized Cu^{2+} moments at the M-I transition.[45] In the insulating state, the fluctuations of local spins at the Cu^{2+} sites produce the relaxation process. As for the DMe- and DMeO-salts (group I), ^{1}H–T_1^{-1} shows a broad peak at 65 K for the DMe-salt and 170 K for the DMeO-salt due to the contribution of the thermally activated methyl rotations.[46] At lower temperatures, where the rotational contribution to the relaxation rate is expected to die out exponentially, ^{1}H–T_1^{-1} does not follow the Korringa-low for both salts. Under pressure, a discontinuous increase of ^{1}H–T_1^{-1} at the M-I transition can be observed.[45] This indicates that the pressure-induced M-I transition is also accompanied by the appearance of localized spins.

The arrangement of Cu^+ and Cu^{2+} ions in the insulating phase can be determined almost uniquely from the average low-temperature crystal structure (Fig. 11).[22] In this model, the nearest-neighbor Cu^{2+} ions (A, B) interact with each other via two DCNQI molecules [Q(1), Q(2)] and the spins

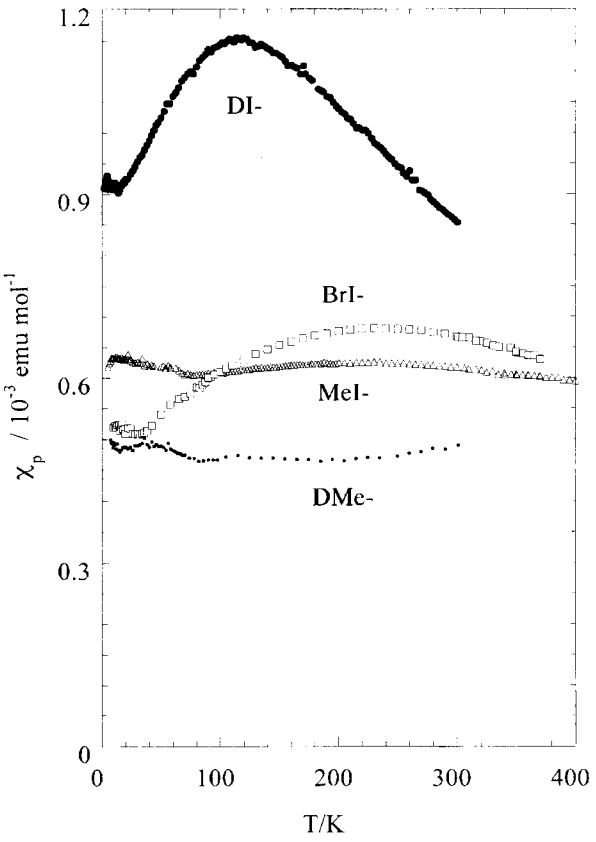

Fig. 10. Temperature dependences of the paramagnetic susceptibility χ_p for the iodine-containing group I salts.

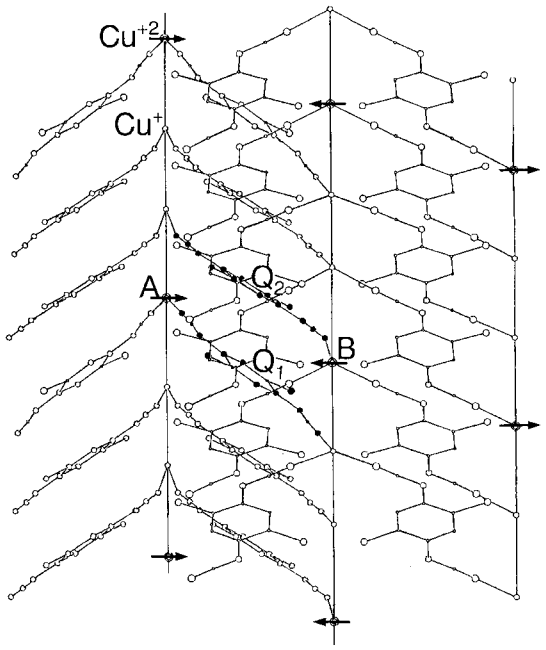

Fig. 11. Arrangement of Cu^+ and Cu^{2+} ions in the insulating phase.

along the *c* axis are parallel to each other. This model has been confirmed by a ^{1}H NMR study.[47] Antiferromagnetic resonance was observed in a single crystal of the group II salt (DMe-DCNQI-d_7[3,3;1])$_2$Cu ($T_N \approx 6.7$ K) which has a unique crystallographic ^{1}H site and is very suitable for the ^{1}H NMR study. Below T_N, the resonance line is split into three pairs of peaks, which is naturally understood by the array along the *c*-axis as $\cdots Cu^{2+}Cu^{+}Cu^{+}\cdots$ and an existence of two sublattices in the ordered antiferromagnetic state. The angular dependence of the pair separations is well explained by the model proposed by the X-ray structure analysis. This result is consistent with that obtained from powdered samples of the DMe-salt under pressure and the DBr-salt. The easy axis is in the *ab*-plane. On rotating the field within the *ab*-plane, minima of the resonance field appear for the field directions parallel to the projections of the Cu–N bonds on to the *ab*-plane. This indicates that the orientation of the spins is governed by the coordination geometry around the Cu ion. Since there are two nonequivalent Cu^{2+} sites in the insulating state, the canting of the spins can be naturally understood. ^{13}C NMR study on the selectively deuterated DMe-salt (–d_6[3,3;0]) with ^{13}C-enriched –C≡N sites indicates that in the insulating state the spins are localized at the Cu^{2+} sites exclusively and the other Cu and DCNQI sites are completely nonmagnetic.[14a]

Pressure dependence of the Néel temperature T_N was studied by NMR for the DMe-salt.[48] It has been revealed that an application of pressure shifts T_N downward: T_N = 8 K (1.5 kbar), 7 K (4.5 kbar), 5.5 K (8.5 kbar). It should be mentioned that the DI-salt in the high-pressure insulating state exhibits the highest T_N (30 K at 16 kbar).[48]

The reentrant transition was investigated by ^{1}H NMR for (DMe-DCNQI-d_2[1,1;0])$_2$Cu and (DMe-DCNQI-d_3 [1,1;1])$_2$Cu.[49] In the reentrant metallic phase, ^{1}H–T_1^{-1} does not follow the Korringa-law, as is observed in the non-deuterated DMe-salt. $(T_1T)^{-1}$ in the reentrant metallic phase is smoothly connected to the extrapolation from the high-temperature side. From the viewpoint of ^{1}H NMR, the insulating state in the group III salts is identical with that in the group II salts and the reentrant metallic phase is essentially the same as the high-temperature metallic phase.

The systematic ^{63}Cu NMR measurements were performed for the DMe- and DMeO-salts (group I), the DBr-salt (group II), and (DMe-DCNQI-d_2[1,1;0])$_2$Cu (group III).[50] In the metallic state, ^{63}Cu–T_1^{-1} follows approximately the Korringa-low for all salts except for the DMe-salts where $(T_1T)^{-1}$ is temperature dependent above 100 K being scaled to the square of the d-spin part of the Knight shift. The analyses of T_1^{-1} and the Knight shift in the metallic state suggest that the density of states at the Fermi level increases in order of the DMeO-salt < the DMe-salt < the DBr-salt. At the M-I transition, both of T_1^{-1} and the Knight shift change discontinuously. The NMR intensity in the insulating phase is decreased to two-thirds of that in the metallic phase. One-third of the Cu NMR signal from Cu^{2+} is anticipated to be out of observation due to the large relaxation rate. This is consistent with the charge separation at the Cu sites ($\cdots Cu^{2+}Cu^{+}Cu^{+}\cdots$).

As for the group III salt, the ^{63}Cu NMR spectrum in the reentrant metallic phase is the same as that in the high-temperature metallic phase, and also the same as that of the non-deuterated DMe-salt.

6. Photoemission Spectroscopy —Mixed Valency of Cu—

Photoemission spectroscopy played an important role in the study of the valence state of Cu.[51] If the Cu ions are in a mixed valence state, the X-ray photoemission spectroscopy (XPS) spectra of the Cu 2p core level should show satellite structures characteristic of the Cu^{2+} state. Since the photoelectron spectroscopy is very surface-sensitive, it is very important to remove Cu^{2+} species in surface contaminations. In order to obtain fresh and clean surfaces, the surface layers of single crystals were removed by gentle scraping with a diamond file in the ultrahigh-vacuum chamber. The Cu 2p spectrum of the DMe-salt measured at ca. 80 K was decomposed into Cu^{+} and Cu^{2+} components by a least-squares line-shape analysis method. The overlapping plasmon-loss satellites accompanying the photoemission peaks were taken into account based on the electron-energy-loss spectroscopy (EELS). The ratio of Cu^{+} to Cu^{2+} is found to be 2 : (0.9±0.1). This indicates that the Cu ion is in a mixed valence-fluctuating state in the metallic phase. The N 1s core-level XPS peak can be decomposed into three peaks (*a*, *b*, and *c*) with the intensity ratio of (approximately) 3 : 2 : 1. The peak *a* is from the imino-nitrogen, the peak *b* is from the cyano-nitrogen coordinating Cu^{+}, and the peak χ is from the cyano-nitrogen coordinating Cu^{2+}. This is again consistent with the Cu^{+} : Cu^{2+} ratio of ca. 2 : 1.

A comparative XPS study of the DMe-, MeBr-, MeCl-, DI-salts was carried out for in-situ synthesized thin film of polycrystals at room temperature.[52] Line shape analyses of the Cu 2p core level spectra indicate that the average valence of Cu shows a systematic change: MeBr- (+1.32) ≈ MeCl- (+1.31) > DMe- (+1.28) > DI- (+1.22). An important point is that the average valence of Cu deviates from the value +1.33 (+4/3) expected from the Cu^{+} : Cu^{2+} ratio = 2 : 1 in the insulating phase. This deviation toward Cu^{+} is enhanced in the group I salts. Furthermore, the further the average valance of Cu deviates away from +4/3, the more difficult it is for the M-I transition to occur. This point will be discussed in detail in Sect. 8-2.

Temperature-dependence of the XPS spectra of the Cu 2p core level was studied for the DI-, MeBr-, and MeCl-salts.[52] In the metallic phase, the Cu 2p spectra are almost temperature-independent above $T_{M\text{-}I}$. In the case of the MeCl-salt ($T_{M\text{-}I}$ = 210 K), the line shape analysis indicates that the Cu^{+} : Cu^{2+} ratio changes from 2 : 0.9 (at 300 K) to 2 : 1.0 (at 170 K), respectively, i.e., the average valence changes from +1.31 (at 300 K) to +4/3 (at 170 K). This suggests that the charge transfer from Cu to DCNQI occurs across the M-I transition.

The existence of a clear Fermi edge in the photoemission spectra of low dimensional materials is an issue of interest. For (DMe-DCNQI-d_7[3,3;1])$_2$Cu ($T_{M\text{-}I}$ = 77 K),

valence-band photoemission spectra with the energy resolution of ca. 40 meV exhibit a power-law dependence on the electron binding energy $|\omega|$ on a high-energy scale (0.3 eV $\leq |\omega| \leq$ 0.05 eV) at high temperatures.[53] This behavior can be interpreted by the single-particle spectral function of a Luttinger liquid[54] near the Fermi level. On the other hand, the spectra for the metallic phase at low temperatures, particularly that taken at 190 K, show a weak but finite intensity at the Fermi level. This indicates the weak 3D character of the conduction electrons and the crossover from a 1D Luttinger liquid to a 3D Fermi liquid with decreasing temperature. The spectrum at 55 K is suppressed near the Fermi level compared to those taken in the metallic phase, which clearly indicates the opening of a gap of at least ca. 0.1 eV in the insulating phase.

Temperature dependence of photoemission spectra in the valence-band region of (DMe-DCNQI-d_2[1,1;0])$_2$Cu (group III) shows that the spectral weight in the vicinity of the Fermi level decreases systematically upon decreasing temperature below the mean-field (MF) transition temperature ($T_{MF} \sim 4T_{M\text{-}I}$) even in the metallic state, resulting in a pseudogap formation above $T_{M\text{-}I}$.[55] This behavior continues across $T_{M\text{-}I}$ and causes the M-I transition. An important observation is that the spectral weight is transferred to higher energies over an energy range much larger than the gap. This indicates that a cooperative effect of strong electron correlation and structural changes is responsible for the changes in the density of state as a function of temperature.

7. Optical Properties

The infrared spectra also indicate the mixed-valence state of the Cu ion. The electron transferred from Cu is accommodated in the lowest unoccupied molecular orbital (LUMO) of DCNQI with antibonding nature on the C=N (imine) and C=C bonds. Therefore, the strength of these bonds is reduced and their stretching frequencies decrease as the electron transfer from Cu to DCNQI proceeds. At room temperature, the wave numbers of infrared absorption bands (ν_i) of neutral DMe- and DBr-DCNQI molecules and their Li and Ba salts are linearly correlated with the degree of the electron transfer (δ).[56] These $\nu_i - \delta$ relations indicate that the δ value for the Cu salts is about 2/3 (therefore, the valence of Cu is +4/3), which is consistent with results of other experiments. For the powdered sample of the DBr-salt below $T_{M\text{-}I}$, the ordinary infrared bands observed at room temperature split into three bands. This splitting is due to an inhomogeneous charge distribution in the DCNQI column produced by the freezing of CDW. The totally symmetric modes observed in the Raman spectra of neutral DCNQI becomes IR-active approximately at $T_{M\text{-}I}$, indicating that the DCNQI molecules deviates from inversion symmetry points in the crystal. The absorption intensities of these modes grow gradually with lowering temperature. This seems to suggest a gradual structural change in the DCNQI columns. But polarized infrared reflectance spectra for the single crystal of (DMe-DCNQI-d_7[3,3;1])$_2$Cu (group II) under almost stress-free condition exhibit the following drastic changes within narrow temperature region around $T_{M\text{-}I}$: 1) the Drude-like dispersion completely disappears in both $E_{//c}$ and $E_{\perp c}$ spectra (c: the stacking axis); 2) a dispersion due to charge-transfer excitation appears in the $E_{//c}$ spectrum; 3) sharp peaks due to electron-molecular vibration coupling appear in the $E_{//c}$ spectrum.[57] The spectrum shows little change below $T_{M\text{-}I}$. These observations indicate that the M-I transition is accompanied by abrupt CDW formation at $T_{M\text{-}I}$. Considering that the electronic state is sensitive to the pressure, one of the possible origins for the gradual behavior observed in the powdered sample in KBr disk is a local-stress effect which leads to a coexistence of the metallic and insulating phases.

It should be noted that the $E_{\perp c}$ reflectance spectrum of the DMe-salt exhibits the strong dispersion, which is the most substantial difference from those of the Ag and Na salts.[58] This dispersion which becomes more remarkable at low temperature can be assigned to the intra-band transition along the inter-column direction. This result means that the conduction band is formed not only along the DCNQI column but also in the inter-column direction. That is, the reflectance spectrum demonstrates the 3D nature of the conduction band.

8. Electronic State —pπ-d Interaction—

8-1. Coexistence of One- and Three-dimensional Fermi Surfaces. The mixed valence state of the Cu ion (Cu^+ : $Cu^{2+} \approx 2 : 1$) in the metallic state implies an interaction between the organic pπ electron and the d electron near the Fermi level. This feature provides very unique electronic structure. The band structure can be depicted using the simple tight-binding approximation. In this calculation, the body-centered unit cell ($\boldsymbol{a}$, $\boldsymbol{b}$, $\boldsymbol{c}$) is reduced to the primitive cell ($\boldsymbol{a}_p$,$\boldsymbol{b}_p$,$\boldsymbol{c}_p$), where $\boldsymbol{a}_p = \boldsymbol{a}$, $\boldsymbol{b}_p = (\boldsymbol{a}+\boldsymbol{b}+\boldsymbol{c})/2$, $\boldsymbol{c}_p = \boldsymbol{c}$ (Fig. 1). The primitive unit cell contains two Cu ions and four DCNQI molecules. For the calculation, the LUMO of DCNQI and the highest-lying d_{xy} orbital of Cu are considered. The band energy $\varepsilon(\boldsymbol{k})$ is obtained from this equation:

$$\begin{vmatrix} 2t_c\cos\boldsymbol{kc}-\varepsilon & 0 & t_a+t_a e^{-i\boldsymbol{kb}} & t_a e^{-i\boldsymbol{ka}}+t_a e^{-i\boldsymbol{kb}} & t_d e^{i\boldsymbol{k}(-\boldsymbol{b}+\boldsymbol{c})} & t_d e^{i\boldsymbol{k}(-\boldsymbol{a}-\boldsymbol{c})} \\ * & 2t_c\cos\boldsymbol{kc}-\varepsilon & t_a+t_a e^{i\boldsymbol{k}(\boldsymbol{a}-\boldsymbol{b}+\boldsymbol{c})} & t_a+t_a e^{i\boldsymbol{k}(-\boldsymbol{b}+\boldsymbol{c})} & t_d e^{i\boldsymbol{kc}} & t_d e^{-i\boldsymbol{kb}} \\ * & * & 2t_c\cos\boldsymbol{kc}-\varepsilon & 0 & t_d e^{-i\boldsymbol{kc}} & t_d e^{i\boldsymbol{k}(-\boldsymbol{a}+\boldsymbol{c})} \\ * & * & * & 2t_c\cos\boldsymbol{kc}-\varepsilon & t_d e^{-i\boldsymbol{kc}} & t_d e^{i\boldsymbol{kc}} \\ * & * & * & * & \Delta-\varepsilon & 0 \\ * & * & * & * & * & \Delta-\varepsilon \end{vmatrix} = 0,$$

where t_c, t_a, and t_d are transfer integrals (LUMO$\cdots$LUMO (intra-stack), LUMO$\cdots$LUMO (inter-stack), LUMO$\cdots d_{xy}$, respectively), Δ is the energy difference between LUMO and d_{xy} ($\Delta = \varepsilon(d_{xy}) - \varepsilon(\text{LUMO})$), and the symbol * expresses complex conjugate.[8b] In the DMe-DCNQI salt, t_a is negligible and we can obtain the analytical solution

$$\varepsilon_{1,2} = 2t_c \cos \boldsymbol{kc},$$

$$\varepsilon_{3,4,5,6} = \frac{\Delta + 2t_c \cos \boldsymbol{kc}}{2} \pm \sqrt{\left(\frac{\Delta - 2t_c \cos \boldsymbol{kc}}{2}\right)^2 + t_d^2(4 \pm \sqrt{D})},$$

where

$$D = 4 + 2[\cos \boldsymbol{k}(\boldsymbol{a} - \boldsymbol{b} - 3\boldsymbol{c}) + \cos \boldsymbol{ka} + \cos \boldsymbol{k}(\boldsymbol{a} - \boldsymbol{b} + 4\boldsymbol{c}) + \cos \boldsymbol{k}(\boldsymbol{b} - 4\boldsymbol{c}) + \cos \boldsymbol{k}(\boldsymbol{b} + 3\boldsymbol{c}) + \cos \boldsymbol{k}(\boldsymbol{a} - 2\boldsymbol{b} + \boldsymbol{c})].$$

The energy band includes purely 1D pπ bands (ε_1, ε_2) which are doubly degenerate. The term Δ is an origin of the 3D dispersion and its contribution is governed by the pπ-d interaction t_d. The calculated band structure and Fermi surface are shown in Fig. 12. The Fermi surface (FS) is composed of two types of sheets (FS1 and FS2) and a connected "arm" with 3D character (FS3). FS1 has a purely pπ character, which is consistent with the CDW instability of the group II and III salts. FS2 is also associated with the pπ band, but is warped due to the pπ-d interaction. FS2 touches FS3 at points designated Q.

This calculation well explains the result of the de Haas-van Alphen (dHvA) experiments for the DMe-salt.[8a] The dHvA measurements were carried out by a standard field modulation technique. Seven different low-frequency (< 3000 T) oscillations with heavy cyclotron masses (3.0—6.5m_o where m_o is free-electron mass) are observed. The dHvA frequency is proportional to the area of a maximal or minimal cross-section of the Fermi surface normal to the magnetic field. The calculated angular dependences for closed orbits on FS3 are in good agreement with those for all the low-frequency oscillations. For the magnetic field higher than 3000 T, many oscillations are detected when the magnetic field is parallel to the *ab* plane. These high-frequency oscillations can be explained in terms of the cyclotron orbits extending over FS2 and FS3 via the points Q, because FS2 and FS3 touch at the points Q. This demonstrates a coexistence of the (quasi) 1D and 3D Fermi surfaces.

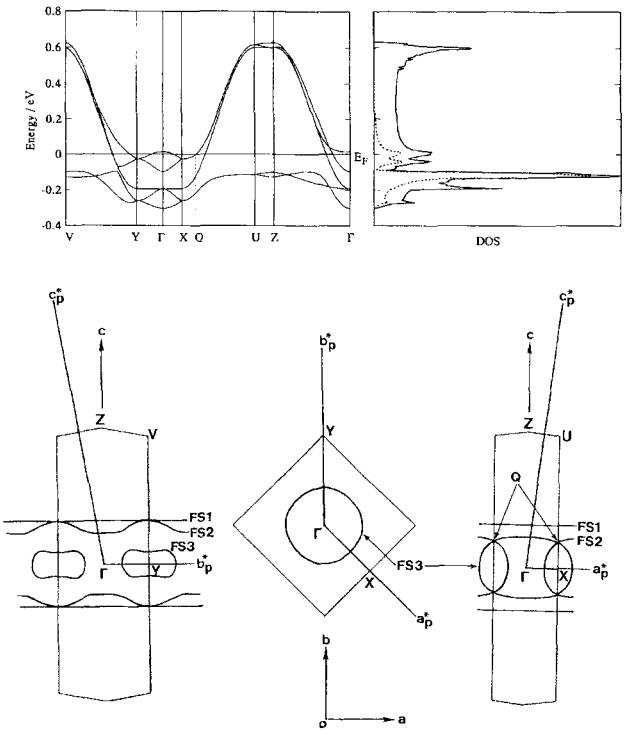

Fig. 12. Calculated band structure, density of states (DOS), and Fermi surface of (DMe-DCNQI)$_2$Cu. Dotted line in DOS indicates contribution from the Cu d_{xy} component.

Although recent Fermi surface studies on the two-dimensional (2D) pπ electron systems are confirming the availability of the tight-binding band calculation for the description of the electronic structure of molecular conductors, its limit of application remains unclear. The above results indicate that this method is applicable even to the pπ-d hybridizing system with complicated 3D character and warrant its wide use. The first-principles calculations based on the local density approximation (LDA) and the generalized gradient approximation (GGA) on the density function theory have been performed for the DMe-salt.[59] The Fermi surfaces obtained by the first-principles calculations agree with the above-mentioned Fermi surfaces.

The density of states at the Fermi level is enhanced by the mixing of pπ and d orbitals and gives ca. 80% of the observed value of the magnetic susceptibility. The calculated band masses $\frac{\hbar^2}{2\pi}\frac{\partial A}{\partial \varepsilon}$ (A; the area of the closed orbit in the plane normal to the magnetic field) associated with the small energy dispersion well explain the heavy cyclotron masses observed in the dHvA measurements. The mixing of pπ and d orbitals provides a very substantial contribution to the heavy cyclotron masses observed.

As for the group III salt, much attention is paid to the reentrant metallic phase near the insulating phase because of the possibility of electron mass enhancement. This possibility is considered in connection with the strong electron–electron correlation and/or the strong electron–phonon interaction, since the steeply enhancement of the electronic specific heat coefficient (γ) near the insulating phase was reported in the alloy system.[22] The dHvA effect is also observed in the reentrant metallic phase of the selectively deuterated DMe-salts (–d_2[1,1;0] and –d_4[1,1;2]).[60] It was found that the reentrant metallic phase has the same Fermi surface as that of the non-deuterated system. The observed cyclotron masses are also the same. Theoretical studies suggest the mass enhancement due to the strong electron correlation or the strong electron-phonon interaction in the DMe-system. And this mass enhancement would become remarkable near the insulating phase. But, the results of the dHvA effect do not indicate such a mass enhancement.

8-2. Pressure and Substitution Effects on the M-I Transition.[36] The substitution effect including the deuterium effect is equivalent to the pressure effect (in the low-pressure region) and is considered to be "chemical" pressure. Both effects should be related to a subtle change in the crystal structure. Tables 1 and 2 show that the M-I transition temperature $T_{M\text{-}I}$ for the group II salts and the critical pressure $P_{M\text{-}I}$ for the group I salts are highly correlated to the N–Cu–N coordination angle α. As shown in Fig. 8, the

phase transitions in the DCNQI-Cu system are accompanied by discontinuous changes of α value. All these facts indicate that the electronic state of the DCNQI-Cu system is interrelated to the distortion of the coordination tetrahedron around the Cu ion.

Since the local spin of Cu^{2+} in the insulating phase indicates the strong Coulomb interaction, the M-I transition in the presence of the strongly correlated states has been studied theoretically.[61] The periodic Anderson model with the electron–phonon interaction has been examined.[62] The fact that the M-I transition is triggered by the Peierls transition has been shown by treating the on-site repulsive interaction within the conventional Hartree–Fock approximation. In the presence of the strong correlation, this Peierls transition is accompanied by the Mott transition associated with the Cu 3d-band, resulting in the localized magnetic moments. By applying the slave-boson theory, the effect of the strong correlation on the electronic state has been demonstrated explicitly.[61d,61e]

The lattice distortion in the insulating phase always exhibits $3c$ periodicity. This is associated with the CDW formation on the DCNQI column and the static charge ordering at the Cu sites ($\cdots Cu^{+}Cu^{+}Cu^{2+}\cdots$) along the c axis. Theoretical studies indicate that an interplay of the three-fold periodic potential and the strong correlation leads to the first-order M-I transition followed by the large hysteresis and the localized spin. It should be noticed that the $3c$ periodicity is a special point where both the CDW and the charge ordering possess the same period.[26] Such a situation yields a large energy gain due to the commensurability between the pπ- and d-systems. Therefore, a deviation of the valence of Cu (DCNQI) from $+4/3$ ($-2/3$) should require the redistribution of the charge for the M-I transition and lower the transition temperature $T_{M\text{-}I}$.

The result of XPS study implies that the formal charge of Cu in the metallic phase is slightly smaller than $+4/3$ and the amount of charge transfer from Cu to DCNQI in the group II salt is larger than that in the type I salt. In the doping effect on the (DMe-DCNQI-d_7[3,3;1])$_2$Cu (group II), the Zn^{2+}-doping at the Cu site slightly raises $T_{M\text{-}I}$, while the Li^{+}-doping lowers it. In the non-deuterated DMe-salt (group I), the Zn^{2+}-doping induces the weak reentrant behavior. On the other hand, the Li^{+}-doping does not affect the metallic behavior except for the increase in the residual resistance. These results suggest that the amount of charge transfer is strongly correlated to $T_{M\text{-}I}$.

The next step is to consider an interrelation between the distortion of the coordination tetrahedron and the charge transfer amount (therefore the valence of Cu). In the tetrahedral coordination geometry with T_d symmetry, the 3d levels are split into t_{2g} (d_{xy}, d_{yz}, d_{zx}) and e_g (d_{z^2}, $d_{x^2-y^2}$) subgroups. A distortion toward D_{4h} symmetry raises the d_{xy} level in the t_{2g} set and lowers the d_{yz} and d_{zx} levels. The highest-lying d_{xy} level is located near the Fermi level and interacts with the pπ band. Therefore, the distortion associated with the pressure or size effect induces small extra electron transfer from Cu to DCNQI and increases the formal charge of Cu.

The pressure and substitution effects on the M-I transition are then summarized as follows:

(1) The valence of Cu in the metallic state is slightly smaller than $+4/3$. This shift of the Cu valence from $+4/3$ stabilizes the metallic state.

(2) The application of pressure or the smaller substituent enhances the distortion of the coordination tetrahedron.

(3) The distortion raises the highest-lying d_{xy} level and induces extra charge transfer from Cu to DCNQI.

(4) The valence state of Cu closer to $+4/3$ provokes the first-order M-I transition triggered by the CDW formation in the presence of the strong correlation.

The point is that the amount of charge transfer is an essential factor which governs the stability of the metallic state.

8-3. Higher-Pressure Metallic Phases and Related Phenomena. As mentioned in the previous section, the first-order M-I transition accompanied by the CDW formation on the DCNQI columns and the static charge ordering at the Cu sites is understood in terms of the amount of charge transfer, which can be tuned by the effective pressure. In order to explain the higher-pressure metallic phases observed in some DCNQI-Cu salts, however, we must consider another factor. The present data show that the higher-pressure metallic phase appears in the salts which do not contain the methyl or methoxy group(s), that is, the DI-, BrI-, and DBr-salts. In the DMe-, DMeO-, MeBr-, MeI-salts, the higher-pressure metallic phase has never been observed.

One possible parameter that we must consider would be the inter-chain interaction.[19] One typical case is the DI-salt. Compared with the DMe-salt, the DI-salt salts exhibit an enhancement of the inter-stack LUMO$\cdots$LUMO interaction (t_a). This is due to the very short I$\cdots$I distance and the contribution of the iodine atom to the LUMO. The Fermi surface of the DCNQI-Cu salt includes a pair of planar sheets associated with the 1D LUMO band. When t_a is negligible, this 1D band is doubly degenerate. This is the case, for example, with the DMe-salt. The CDW formation that triggers the M-I transition originates from the perfect nesting of this 1D Fermi surface. If the t_a value is enhanced under pressure, the degeneracy would be removed to generate two pairs of corrugated sheets. In this case, the perfect nesting of the Fermi surface becomes difficult. It is plausible that the best nesting vector is no longer $(0,0,c^*/3)$ and thus the CDW formation is not coupled to the charge ordering at the Cu sites. Such a situation would explain the resistivity peak followed by the low-temperature metallic behavior for the DI-salt above 20 kbar. According to this picture, the enhancement of the resistivity above 20 kbar is due to a simple CDW formation with $2k_F \neq c^*/3$ and the 3D Fermi surface (and a part of the corrugated sheets) survives down to the lowest temperature. The low-temperature X-ray diffraction study under pressure for the DI-salt, however, found no superlattice structure in this pressure region.[33b] The X-ray structure analysis for the DI-salt under 25 kbar at room temperature indicates that the inter-column LUMO$\cdots$LUMO interaction is almost unchanged by applying pressure. These results seem to cast doubt on the role of the inter-chain interaction.

Table 4. Electronic Specific Heat Coefficient γ for (R_1,R_2-DCNQI)$_2$Cu (group I)

R_1,R_2-DCNQI	γ / mJ K^{-2} mol^{-1}
DMeO-DCNQI	9
DI-DCNQI	70
MeI-DCNQI	30—40
BrI-DCNQI	50—60
DMe-DCNQI	25

Another possibility has been proposed theoretically on the basis of the mean field calculations with the 3-chain and 6-chain periodic Anderson models.[63] In this model, the pressure effect is expressed as the upshift of the d_{xy} level. Depending on various parameters, such as nearest neighbor interactions and inter-chain transfer integrals, the system undergoes the following two types of successive phase transitions as a function of pressure both in the 3-chain and 6-chain models:

(A) Metal → Insulator (with the 3-fold periodicity) → Insulator,

(B) Metal → Insulator (with the 3-fold periodicity) → Metal → Insulator.

The nearest neighbor Coulomb interaction between Cu and DCNQI (V_M) is the crucial parameter for the classification of the types of transitions (A) and (B) noted above. When V_M/t_c (t_c; DCNQI intra-chain transfer integral) is smaller than 0.8, the system undergoes the type (B) transition. The higher-pressure insulating phase is the Mott insulator with the antiferromagnetic ordering in the chain direction. This model well explains the high-pressure metallic phase followed by the insulating phase. Although the relation between the substituents (R_1, R_2) and V_M is not so clear, it may be possible that the feature of LUMO in the iodine-containing DCNQIs extending towards the I atom(s) reduces the V_M value. However, it seems doubtful that this is also the case for the DBr-salt.

For both explanations mentioned above, another model should be introduced in order to understand the metallic state at the highest pressure region. In any case, lack of crucial experimental data hinders clear understanding of the high-pressure electronic states.

9. Thermal Properties

9-1. Mass Enhancement. The electronic specific heat coefficient γ is customarily discussed in terms of the effective mass of the conduction electron. The heavy electron system found in the lanthanoid and actinoid compounds is characterized by the enhancement of γ and χ values. In the early stage of the research, a possibility of the "molecular heavy electron" system was proposed on the basis of the pπ-d mixing state in the DCNQI-Cu salts.[22] Table 4 shows the γ values of the group I salts. The γ value of the DMeO-salt is within range of those for typical organic conductors such as (TMTSF)$_2$ClO$_4$ (γ = 10 mJ K^{-2} mol^{-1}).[64] The DMe-salt shows a slightly enhanced γ value at ambient pressure.[65] As for the DMe-salt, a possibility of the mass enhancement in the reentrant metallic phase was intensively examined. As is the case of the magnetic properties and the dHvA effect, however, the γ value in the reentrant metallic phase of the selectively deuterated DMe-salts is identical with that in the metallic state of the non-deuterated DMe-salt and indicates no mass enhancement due to the many body effect.[65b] On the other hand, the iodine-containing group I salts exhibit rather large γ values.[43] Especially, the γ value of the DI-salt is about three times as large as that of the DMe-salt. In the heavy electron system, the γ value is related to the coefficient of the T^2 term in the resistivity (A) in terms of the Kadowaki–Woods relation, $A/\gamma^2 = 1.0\times10^5$ $\mu\Omega$ cm mol^2 K^2 mJ^{-2}.[66] The γ value derived from this relation (71 mJ K^{-2} mol^{-1}) is very close to that obtained from the specific heat measurement. The theory of the interacting Fermi liquid treats the relation between γ and the susceptibility at 0 K (χ_0) in terms of the Wilson ratio $R_W = (\chi_0/2\mu_B^2)/(3\gamma/2\pi^2k_B^2)$ and experimental R_W values for the heavy electron systems are distributed around 1.[67] The DI-salt gives the Wilson ratio close to 1 (R_W = 0.94). These results suggest that the DI-salt is characterized as a Fermi liquid system with enhanced mass and density of states. As mentioned in Sect. 5-1, the effective pπ-d hybridization is expected to be reduced in the iodine-containing DCNQI-Cu salts, in the framework of the spin fluctuation mechanism. In other salts such as the DMe-salt, the pπ-d hybridization is so strong that the d electrons are merged into the conduction band and well delocalized in the metallic state. On the other hand, the enhanced γ and χ values in the iodine-containing salts suggest an interplay between the d-like electrons and pπ-electrons in the metallic state, so the heavy electron picture may be still alive in this system.

9-2. Antiferromagnetic Transition. Thermal properties of the antiferromagnetic transition in the insulating phase were investigated with use of the fully and selectively deuterated DMe-salts (–d_8, –d_3[3,0;0]; group II) and the alloy [(DMe-DCNQI-h)$_{1-x}$(DMe-DCNQI-d_8)$_x$]$_2$Cu (x = 0.47; group III).[68] The specific heat of the –d_8 salt does not obey the well-known $C/T = \gamma+\beta T^2$ rule. The excess specific heat derived by the subtraction of the lattice contribution shows a maximum around 6.8 K which is very close to T_N (Fig. 13). A possible origin of this excess specific heat is the freedom of the Cu^{2+} spin system. The excess entropy calculated from this excess specific heat is 1.8 J mol^{-1} K^{-1}. The calculated entropy on the assumption that one-third of the Cu atoms are in the Cu^{2+} state, is $(k_BN_A/3)\ln 2$ = 1.9 J mol^{-1} K^{-1} (N_A; the Avogadro number, k_B; Boltzmann constant), which is very close to the experimental value. This spin entropy grows from zero to 1.8 J mol^{-1} K^{-1} across T_N, and stays constant above 18 K. The –d_3[3,0;0] salt, which is the group II salt situated close to the boundary between the group II and group III salts, exhibits the same specific heat behavior as the –d_8 salt. This means that the spin entropy is independent of the chemical pressure.

On the other hand, the reentrant metallic phase of the alloy [(DMe-DCNQI-h)$_{0.53}$(DMe-DCNQI-d_8)$_{0.47}$]$_2$Cu is very close to the insulating phase in the phase diagram. When the sample was cooled with the rate of 1 K min^{-1}, an excess

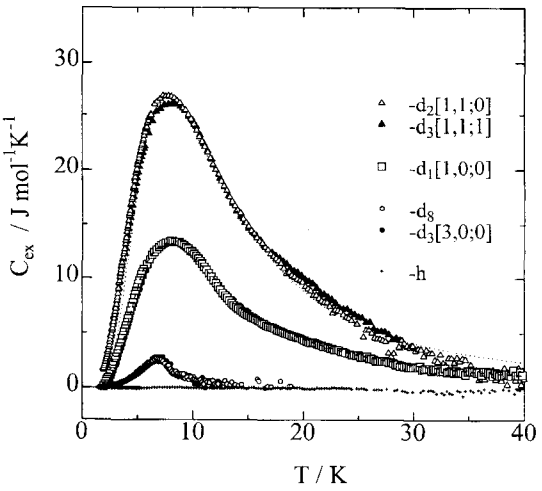

Fig. 13. Excess specific heat C_{ex} for the selective deuterated DMe-salts subtracting the lattice contributions. Dotted and dashed lines are Schottky models, $C_{ex} = Nk_B(\Delta/T)^2(g_0/g_1)\exp(\Delta/T)[1+(g_0/g_1)\exp(\Delta/T)]^2$, where $g_0 = 1$ and $g_1 = 2$ are degeneracies of the ground and first excited states, $\Delta/k_B = 20$ [K] is the energy difference, and $N = 4N_A$ (for dotted line) or $2N_A$ (for dashed line).

specific heat with a peak at 6.8 K and a reduced γ value were observed. Annealing of the sample suppresses the excess entropy and enhances the γ value. All these results indicate that the insulating domain remains within the metallic region in the case of rapid cooling and that the γT term comes only from the metallic state and is not due to the freedom of the Cu^{2+} spins as observed in spin glass systems.

9-3. Reentrant Transition. It has been theoretically proposed that the reentrant transition can be phenomenologically explained by a thermodynamic treatment of a first-order transition, where only the contribution of the Cu^{2+} spin degrees of freedom in the insulating state and that of the conduction electrons in the metallic phase are considered.[61c] For the group III DMe-salts (–d_2[1,1;0] and –d_4[1,1;2]), specific heat and latent heat were measured by thermal relaxation (0.5 K $< T <$ 40 K), adiabatic pulse (20 K $< T <$ 100 K) and differential thermal analysis methods.[65b,69] In the metallic phase, the conduction electron system has the entropy given as γT, whereas the entropy due to the Cu^{2+} spins given as $(k_BN_A/3)\ln 2$ above 18 K is important in the insulating phase. The entropy difference ΔS between the metallic and insulating phases has been determined experimentally and is expressed as $\Delta S = \gamma^* T - S_I$, where $\gamma^* = 40$ mJ mol^{-1} K^{-1} and $S_I = (k_BN_A/3)\ln 2 = 1.9$ J mol^{-1} K^{-1}. This γ^* value is much larger than the γ value for the DMe-salt (25 mJ mol^{-1} K^{-1}), and thus there should be another factor which contributes to the $\gamma^* T$ behavior of ΔS. The lattice vibration is the most plausible candidate, because the lattice specific heat in the temperature region 20 K $< T <$ 100 K shows approximately linear temperature dependence in both the metallic and insulating phases.

The phenomenological theory is applicable, if γ is replaced by γ^*.[69] Above 18 K, the difference of Gibbs free energies ΔG between the metallic and insulating phases is expressed as,

$$\Delta G = \Delta G_o - \frac{1}{2}\gamma^* T^2 + S_I T,$$

where $\gamma^* = 40$ mJ mol^{-1} K^{-1} and

$$S_I = (k_BN_A/3)\ln 2 = 1.9 \text{ J mol}^{-1} \text{ K}^{-1}.$$

All that occur below 18 K are included in the integration constant ΔG_o. This ΔG_o is the only parameter which expresses the difference of the compound and thus is related to the effective pressure. The metallic state appears when ΔG is negative, and the insulating phase appears when ΔG is positive. The transition temperature is given by the equation $\Delta G = 0$. The behavior of the solution depends on ΔG_o. When ΔG_o is largely negative ($\Delta G_o \leq -S_I^2/2\gamma^*$), there is no real solution and ΔG is always negative, which means that the metallic state is stable over all the temperature range. This corresponds to the group I salts. In the condition of $-S_I^2/2\gamma^* \leq \Delta G_o \leq 0$, the equation gives two real and positive solutions, and the system changes as metal→insulator→metal with lowering temperature. This behavior is just that of the group III salts. When ΔG_o is positive, the equation gives one positive solution. The system changes from metal to insulator at this temperature. This behavior corresponds to that of the group II salts. Assuming that ΔG_o is a linear function of the effective pressure, the phase diagram can be reproduced quite well. In conclusion, the reentrant transition is a result of the competition between two temperature-dependent terms in the free energy. One comes from the Cu^{2+} spin system in the insulation phase, whereas the other comes from the conduction electrons in the metallic phase and the lattice vibrations. The difference in the temperature dependence of these two terms plays an essential role in the reentrant transition. The microscopic study of the strong correlation effect on the M-I transition by use of the mean-field theory for the slave-boson has demonstrated the reentrant transition and has explained the pressure–temperature phase diagram.[61c]

9-4. Schottky-Type Specific Heat Anomaly.[70] The specific heat measurements for DMe-salts (group I; –d_1[1,0;0]. group III; –d_3[1,0;2], –d_2[1,1;0], –d_3[1,1;1], –d_4[1,1;2]) with partially deuterated methyl group(s) have revealed an extraordinary excess specific heat (Fig. 13). In contrast to the DMe-salts with non- or fully-deuterated methyl group(s) (–h, –d_8, and –d_3[3,0;0]), the DMe-salts with –CH_2D group-(s) show a Schottky-type giant peak. The excess specific heat value classifies the selective deuterated salts into two groups. In the first group (the –d_2[1,1;0], –d_3[1,1;1], and –d_4[1,1;2] salts), the excess specific heat values are nearly equal to each other and quite large (> 20 J mol^{-1} K^{-1}), whereas in the second group (the –d_1[1,0;0] and –d_3[1,0;2] salts) the maximum specific heat values are reduced to half of those for the first group. This specific heat anomaly is ascribed to the rotation of the deuterated methyl groups (–CH_2D). The ^{1}H NMR study indicates that the methyl rotation needs the excitation energy below ca. 70 K. The deuterium atom in

the $-CH_2D$ group can take three different positions through the quantum tunneling. It should be noticed that the first group salts contain four $-CH_2D$ groups and the second group salts contain two $-CH_2D$ groups within one formula unit $(DME\text{-}DCNQI)_2Cu$. Therefore, the calculated entropies are $S = 4k_BN_A\ln 3 = 36.4\ J\,mol^{-1}\,K^{-1}$ for the first group and $2k_BN_A\ln 3 = 18.2\ J\,mol^{-1}\,K^{-1}$ for the second group, respectively. The temperature dependences of the excess specific heat can be explained on the assumption that the introduction of the D atom leads to the ground state split into three levels and excitations among these levels give rise to the Schottky like specific heat anomaly. It should be added that the specific heat for the $-d_4$[2,2;0] and $-d_2$[2,0;0] salts which contain the $-CHD_2$ group instead of the $-CH_2D$ group cannot be explained in terms of the Schottky-type anomaly.[71] The reason is an open question.

10. Conclusion

Development of molecular conductors for the last two decades has proceeded on two major trends:

(1) From "*one-dimensional*" to "*higher-dimensional*"

(2) From "*single component*" to "*multi component*".[72]

At first, the molecular metal was the 1D metal. KCP and TTF-TCNQ are typical examples. The 1D metal cannot retain the metallic state down the low-temperature region due to the instability of the planar Fermi surface. Therefore, much effort to increase the dimensionality of the electronic structure has been made by means of chemical modification. The first organic superconducting system, $(TMTSF)_2X$, forms a quasi-1D system as a result of the introduction of Se atoms into the TTF moiety. The BEDT-TTF salts, the second-generation organic superconductors, have gained various types of strong 2D characters through the six-membered heterorings joined to the TTF moiety. And, the DCNQI-Cu salt is the first molecular conductor with the 3D Fermi surface. This 3D nature is brought about by the tetrahedral coordination geometry around the Cu ion and the pπ-d mixing, which was never observed in the conventional molecular conductors.

From another point of view, molecular conductors at the first stage were classified into a "*single component*" system where only one degree of freedom governs transport properties. Recently, however, an increasing number of interesting systems which have "two" bands with different characters near the Fermi level, or where itinerant pπ electrons interact with localized d spins, have been reported. Such "*multi component*" systems exhibit interesting physical properties derived from an interplay of various components. The DCNQI-Cu system where the pπ electrons coexist with itinerant d electrons is a typical example.

As shown in the present account, the DCNQI-Cu salts have played an important role in both trends. The DCNQI-Cu salts show a variety of physical properties: the CDW, the Mott transition, the mixed-valence state, the pressure-induced M-I transition, the reentrant transition, the 3D Fermi surface, the anomalous isotope effects, the antiferromagnetic transition, the weak ferromagnetisim, the mass enhancement, and the Schottky-type specific heat anomaly. It is surprising that almost all of them are exquisitely stage-managed phenomena played out by a couple of pπ and d electrons. The *simplicity* and *variety* observed in the DCNQI-Cu system demonstrate a prominent feature of the molecular conductor. Finally, it should be emphasized that there still remain many unsettled problems in this system. They include the origin of the high-pressure metallic phase, details of the three-fold superstructure in the insulating phase, specific heat anomaly in the selectively deuterated DMe-salts, origin of the heavy atom isotope effect, and the mechanism of mass enhancement in the iodine-containing salts.

The author would like to express his sincere thanks to Prof. H. Kobayashi (Institute for Molecular Science), Prof. A. Kobayashi (University of Tokyo), Prof. T. Mori (Tokyo Institute of Technology), Dr. S. Aonuma (Institute for Solid State Physics, University of Tokyo), Prof. H. Sawa (Chiba University), Dr. Y. Kashimura (Institute for Solid State Physics, University of Tokyo), Prof. M. Kinoshita (Science University of Tokyo in Yamaguchi), Dr. M. Tamura (Toho University), Prof. Y. Nishio (Toho University), Prof. S. Kagoshima (University of Tokyo), Prof. T. Takahashi (Gakushuin University), Prof. Y. Kitaoka (Osaka University), Dr. S. Uji (National Research Institute for Metals), Prof. A. Fujimori (University of Tokyo), Prof. T. Takahashi (Tohoku University), Prof. M. Tasumi (Saitama University), Prof. H. Tajima (Institute for Solid State Physics, University of Tokyo), and Prof. K. Yakushi (Institute for Molecular Science) who contributed to the chemistry and physics of the DCNQI-Cu system presented in this account.

This work was partially supported by Grants-in-Aid for Scientific Research on Priority Area "Metal-assembled Complexes" (Area No. 401/10149103) and "Novel Electronic States in Molecular Conductors" (Area No. 253/06243105) from the Ministry of Education, Science, Sports and Culture.

References

1 H. Akamatsu, H. Inokuchi, and Y. Matsunaga, *Nature*, **173**, 168 (1954).

2 L. B. Coleman, M. J. Cohen, D. J. Sandman, F. G. Yamagishi, A. F. Garito, and A. J. Heeger, *Solid State Commun.*, **12**, 1125 (1973).

3 a) K. Bechgaard, C. S. Jacobsen, K. Mortensen, H. J. Pedersen, and N. Thorup, *Solid State Commun.*, **33**, 1119 (1980). b) D. Jérome, A. Mazaud, M. Ribault, and K. Bechgaard, *J. Phys. Lett.*, **41**, L95 (1980).

4 J. Wosnitza, "Fermi Surfaces of Low-Dimensional Organic Metals and Superconductors," Springer Tracts in Modern Physics, Vol. 134, Springer (1996).

5 A. Aumüller, P. Erk, G. Klebe, S. Hünig, J. U. von Schütz, and H-P. Werner, *Angew. Chem., Int. Ed. Engl.*, **25**, 740 (1986).

6 a) R. Kato, H. Kobayashi, A. Kobayashi, T. Mori, and H. Inokuchi, *Chem. Lett.*, **1987**, 1579. b) S. Hünig and P. Erk, *Adv. Mater.*, **3**, 225 (1991). c) S. Hünig, M. Kemmer, H. Meixner, K. Sinzger, H. Wenner, T. Bauer, E. Tillmanns, F. R. Lux, M. Hollstein, H-G. Groß, U. Langohr, H-P. Werner, J. U. von Schütz, and H. C. Wolf, *Eur. J. Inorg. Chem.*, **1999**, 899.

7 A. Kobayashi, R. Kato, H. Kobayashi, T. Mori, and H.

Inokuchi, *Solid State Commun.*, **64**, 45 (1987).

8 a) S. Uji, T. Terashima, H. Aoki, J. S. Brooks, R. Kato, H. Sawa, S. Aonuma, M. Tamura, and M. Kinoshita, *Phys. Rev. B*, **50**, 15597 (1994). b) R. Kato, S. Aonuma, and H. Sawa, *Synth. Met.*, **70**, 1071 (1995).

9 a) T. Mori, K. Imaeda, R. Kato, A. Kobayashi, H. Kobayashi, and H. Inokuchi, *J. Phys. Soc. Jpn.*, **56**, 3429 (1987). b) S. Tomić, D. Jérome, A. Aumüller, P. Erk, S. Hünig, and J. U. von Schütz, *Eur. Phys. Lett.*, **5**, 553 (1988).

10 S. Tomić, D. Jérome, A. Aumüller, P. Erk, S. Hünig, and J. U. von Schütz, *J. Phys. C: Solid State Phys.*, **21**, L203 (1988).

11 R. Kato, H. Kobayashi, and A. Kobayashi, *J. Am. Chem. Soc.*, **111**, 5224 (1989).

12 a) S. Hünig, K. Sinzger, M. Jopp, D. Bauer, W. Bietsch, J. U. von Schütz, and H. C. Wolf, *Angew. Chem., Int. Ed. Engl.*, **31**, 859 (1992). b) K. Sinzger, S. Hünig, M. Jopp, D. Bauer, W. Bietsch, J. U. von Schütz, H. C. Wolf, R. K. Kremer, T. Metzenthin, R. Bau, S. I. Khan, A. Lindbaum, C. L. Lengauer, and E. Tillmanns, *J. Am. Chem. Soc.*, **115**, 7696 (1993).

13 a) A. Aumüller and S. Hünig, *Angew. Chem., Int. Ed. Engl.*, **23**, 447 (1984). b) A. Aumüller and S. Hünig, *Liebigs. Ann. Chem.*, **1986**, 142. c) S. Hünig, R. Bau, M. Kemmer, H. Meixner, T. Metzenthin, K. Peters, K. Sinzger, and J. Gullbis, *Eur. J. Org. Chem.*, **1998**, 335.

14 a) A. Kawamoto, K. Miyagawa, and K. Kanoda, *Phys. Rev. B*, **58**, 1243 (1998). b) K. Miyagawa, A. Kawamoto, and K. Kanoda, *Phys. Rev. B*, **60**, 14847 (1999).

15 S. Aonuma, H. Sawa, and R. Kato, *J. Chem. Soc., Perkin Trans. 2*, **1995**, 1541.

16 a) R. Kato, S. Aonuma, H. Sawa, K. Hiraki, and T. Takahashi, *Synth. Met.*, **68**, 195 (1995). b) S. Aonuma, H. Sawa, and R. Kato, *Mol. Cryst. Liq. Cryst.*, **285**, 163 (1996). c) S. Aonuma and R. Kato , *Synth. Met.*, **102**, 1749 (1999).

17 a) R. Kato, Y. Kashimura, S. Aonuma, H. Sawa, H. Takahashi, and N. Môri, *Mol. Cryst. Liq. Cryst.*, **285**, 143 (1996). b) Y. Kashimura, Doctor Thesis, The University of Tokyo (1999).

18 T. Mori, H. Inokuchi, A. Kobayashi, R. Kato, and H. Kobayashi, *Phys. Rev. B*, **38**, 5913 (1988).

19 Y. Kashimura, H. Sawa, S. Aonuma, R. Kato, H. Takahashi, and N. Môri, *Solid State Commun.*, **93**, 675 (1995).

20 R. T. Henriques, W. Kang, S. Tomić, D. Jérome, P. Erk, S. Hünig, and J. U. von Schütz, *Solid State Commun.*, **68**, 909 (1988).

21 a) H. Kobayashi, A. Miyamoto, R. Kato, A. Kobayashi, Y. Nishio, K. Kajita, and W. Sasaki, *Solid State Commun.*, **72**, 1 (1989). b) K. Murata, M. Ishibashi, N. A. Fortune, A. Kobayashi, R. Kato, and H. Kobayashi, *Synth. Met.*, **41—43**, 2487 (1991).

22 H. Kobayashi, A. Miyamoto, R. Kato, F. Sakai, A. Kobayashi, Y. Yamakita, Y. Furukawa, M. Tasumi, and T. Watanabe, *Phys. Rev. B*, **47**, 3500 (1993).

23 H. Sawa et al., private communication.

24 A. Kobayashi, R. Kato, and H. Kobayashi, *Chem. Lett.*, **1989**, 1843.

25 H. Kobayashi, A. Miyamoto, H. Moriyama, R. Kato, and A. Kobayashi, *Chem. Lett.*, **1991**, 863.

26 R. Kato, H. Sawa, S. Aonuma, Y. Okano, S. Kagoshima, A. Kobayashi, and H. Kobayashi, *Synth. Met.*, **56**, 1864 (1993).

27 H. Sawa, M. Tamura, S. Aonuma, R. Kato, and M. Kinoshita, *J. Phys. Soc. Jpn.*, **63**, 4302 (1994).

28 R. Kato, H. Sawa, S. Aonuma, M. Tamura, M. Kinoshita, and H. Kobayashi, *Solid State Commun.*, **85**, 831 (1993).

29 S. Aonuma and R. Kato, to be submitted.

30 S. Kagoshima, H. Nagasawa, and T. Sambongi, "One-Dimensional Conductors," Springer Series in Solid-State Sciences 72, Springer-Verlag, Berlin and Heidelberg (1988).

31 R. Moret, P. Erk, S. Hünig, and J. U. von Schütz, *J. Phys. Paris*, **49**, 1925 (1988).

32 Y. Nogami, K. Oshima, K. Hiraki, and K. Kanoda, *J. Phys., Colloq.*, in press.

33 a) Y. Nogami, S. Hayashi, T. Date, K. Oshima, K. Hiraki, and K. Kanoda, *Rev. High P. Sci. Technol.*, **7**, 404 (1998). b) Y. Nogami, Y. Yamamoto, S. Hayashi, K. Oshima, K. Hiraki, and K. Kanoda, *Synth. Met.*, **103**, 2252 (1999).

34 H. Kobayashi, H. Sawa, S. Aonuma, and R. Kato, *J. Am. Chem. Soc.*, **115**, 7870 (1993).

35 H. Sawa, M. Tamura, S. Aonuma, R. Kato, M. Kinoshita, and H. Kobayashi, *J. Phys. Soc. Jpn.*, **62**, 2224 (1993).

36 R. Kato, S. Aonuma, and H. Sawa, *Mol. Cryst. Liq. Cryst.*, **284**, 183 (1996).

37 H. Kobayashi, R. Kato, A. Kobayashi, T. Mori, and H. Inokuchi, *Solid State Commun.*, **65**, 1351 (1988).

38 M. Tamura, H. Sawa, S. Aonuma, R. Kato, M. Kinoshita, and H. Kobayashi, *J. Phys. Soc. Jpn.*, **62**, 1470 (1993).

39 M. Tamura, H. Sawa, Y. Kashimura, S. Aonuma, R. Kato, and M. Kinoshita, *J. Phys. Soc. Jpn.*, **63**, 425 (1994).

40 M. Tamura, H. Sawa, S. Aonuma, R. Kato, M. Kinoshita, and H. Kobayashi, *J. Phys. Soc. Jpn.*, **63**, 429 (1994).

41 a) T. Mori, S. Bandow, H. Inokuchi, A. Kobayashi, R. Kato, and H. Kobayashi, *Solid State Commun.*, **67**, 565 (1988). b) H. Kobayashi, R. Kato, A. Kobayashi, Y. Nishio, K. Kajita, and W. Sasaki, *J. Phys. Chem. Solids.*, **51**, 533 (1990).

42 M. Tamura, Y. Kashimura, H. Sawa, S. Aonuma, R. Kato, and M. Kinoshita, *Solid State Commun.*, **93**, 585 (1995).

43 M. Tamura, N. Someya, Y. Nishio, K. Kajita, Y. Kashimura, S. Aonuma, H. Sawa, and R. Kato, *Mol. Cryst. Liq. Cryst.*, **285**, 151 (1996).

44 M. T. Béal-Monod and J. Lawrence, *Phys. Rev. B*, **21**, 5400 (1980).

45 T. Takahashi, K. Kanoda, T. Tamura, K. Hiraki, K. Ikeda, R. Kato, H. Kobayashi, and A. Kobayashi, *Synth. Met.*, **56**, 2281 (1993).

46 K. Kanoda, T. Tamura, T. Ohyama, T. Takahashi, R. Kato, H. Kobayashi, and A. Kobayashi, *Synth. Met.*, **42**, 1843 (1991).

47 K. Hiraki, Y. Kobayashi, T. Nakamura, T. Takahashi, S. Aonuma, H. Sawa, R. Kato, and H. Kobayashi, *J. Phys. Soc. Jpn.*, **64**, 2203 (1995).

48 K. Hiraki et al., unpublished results.

49 K. Hiraki, K. Takagawa, T. Nakamura, T. Takahashi, S. Aonuma, H. Sawa, and R. Kato, *Synth. Met.*, **70**, 1069 (1995).

50 K. Ishida, Y. Kitaoka, H. Masuda, K. Asayama, T. Takahashi, A. Kobayashi, R. Kato, and H. Kobayashi, *J. Phys. Soc. Jpn.*, **64**, 2970 (1995).

51 I. H. Inoue, A. Kakizaki, H. Namatame, A. Fujimori, A. Kobayashi, R. Kato, and H. Kobayashi, *Phys. Rev. B*, **45**, 5828 (1992).

52 O. Akaki, A. Chainani, T. Takahashi, Y. Kashimura, and R. Kato, *Phys. Rev. B*, **57**, 11846 (1998).

53 A. Sekiyama, F. Fujimori, H. Sawa, S. Aonuma, and R. Kato, *Phys. Rev. B*, **51**, 13899 (1995).

54 J. M. Luttinger, *J. Math. Phys.*, **4**, 1154 (1963).

55 T. Takahashi, T. Yokoya, A. Chainani, H. Kumigashira, O. Akaki, and R. Kato, *Phys. Rev. B*, **53**, 1790 (1996).

56 Y. Yamakita, Y. Furukawa, A. Kobayashi, M. Tasumi, R. Kato, and H. Kobayashi, *J. Chem. Phys.*, **100**, 2449 (1994).

57 H. Tajima, S. Aonuma, H. Sawa, and R. Kato, *J. Phys. Soc.*

Jpn., **64**, 2502 (1995).

58 K. Yakushi, A. Ugawa, G. Ojima, T. Ida, H. Tajima, H. Kuroda, A. Kobayashi, R. Kato, and H. Kobayashi, *Mol. Cryst. Liq. Cryst.*, **181**, 217 (1990).

59 T. Miyazaki and K. Terakura, *Phys. Rev. B*, **54**, 10452 (1996).

60 S. Uji, T. Terashima, H. Aoki, R. Kato, H. Sawa, S. Aonuma, M. Tamura, and M. Kinoshita, *Solid State Commun.*, **93**, 203 (1995).

61 a) H. Fukuyama, *J. Phys. Soc. Jpn.*, **61**, 3452 (1992). b) H. Fukuyama, in "Proceedings of the 16th Taniguchi Symposium 1993, Correlation Effects in Low-Dimensional Electron Systems," ed by A. Okiji and N. Kawakami, Springer-Verlag, Berlin (1994), p. 128. c) M. Nakano, M. Kato, and K. Yamada, *Physica B*, **186—188**, 1077 (1993). d) T. Ogawa and Y. Suzumura, *J. Phys. Soc. Jpn.*, **63**, 2066 (1994). e) T. Ogawa and Y. Suzumura, *Phys. Rev. B*, **53**, 7085 (1996).

62 Y. Suzumura and H. Fukuyama, *J. Phys. Soc. Jpn.*, **61**, 3322 (1992).

63 a) C. Hotta and H. Fukuyama, *J. Phys. Soc. Jpn.*, **68**, 941 (1999). b) C. Hotta, *J. Phys. Soc. Jpn.*, **68**, 2703 (1999).

64 Y. Nishio, K. Kajita, W. Sasaki, R. Kato, A. Kobayashi, and H. Kobayashi, *Solid State Commun.*, **81**, 473 (1992).

65 a) S. Kagoshima, A. Miyazaki, T. Osada, Y. Saito, N. Wada, H. Yano, T. Takahashi, K. Kanoda, H. Kobayashi, A. Kobayashi, and R. Kato, *Synth. Met.*, **55—57**, 1832 (1993). b) N. Someya, Y. Nishio, M. Tamura, K. Kajita, S. Aonuma, H. Sawa, R. Kato, and H. Kobayashi, *Synth. Met.*, **86**, 2077 (1997).

66 K. Kadowaki and S. B. Woods, *Solid State Commun.*, **58**, 507 (1986).

67 P. A. Lee, T. M. Rice, J. W. Serene, L. J. Sham, and J. W. Wilkins, *Comments Condens. Mat. Phys.*, **12**, 99 (1986).

68 Y. Nishio, T. Tega, M. Tamura, K. Kajita, S. Aonuma, H. Sawa, R. Kato, and H. Kobayashi, *Synth. Met.*, **85**, 1739 (1997).

69 Y. Nishio et al., *J. Phys. Soc. Jpn.*, in press.

70 Y. Nishio, T. Tega, K. Kajita, H. Kobayashi, S. Aonuma, H. Sawa, and R. Kato, *Synth. Met.*, **71**, 1947 (1995).

71 Y. Nishio, private communication.

72 S. Kagoshima, R. Kato, H. Fukuyama, H. Seo, and H. Kino, in "Advanced in Synthetic Metals-Twenty Years of Progress in Science and Technology-," ed by P. Bernier, S. Lefrant, and G. Bidan, Elsevier, (1999), p. 262.

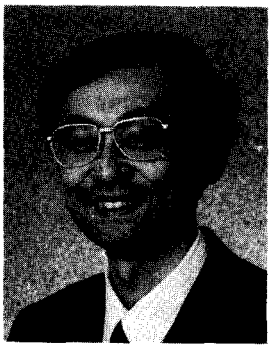

Reizo Kato was born in 1955 in Yamaguchi, Japan. He received his B. Sc. degree in 1979, M. Sc. in 1981 and D. Sc. in 1984 from The University of Tokyo. He was appointed research associate of Department of Chemistry at Toho University in 1984, and he was promoted lecturer in 1988. He jointed the Institute for Solid State Physics in The University of Tokyo as an associate professor in 1990. Since 1999 he has been a chief scientist, a director of "Condensed Molecular Materials" laboratory in RIKEN (The Institute of Physical and Chemical Research). He received Chemical Society of Japan Award for Young Chemists in 1990 and IBM Japan Science Prize in 1995 for his works on molecular conductors. His research has been focused on development of new molecular materials, especially molecular metals and superconductors.